J. Phys. A: Math. Gen. **33** (2000) 2685–2723. Printed in the UK PII: S0305-4470(00)08789-8

On three-dimensional self-avoiding walk symmetry classes

A Rechnitzer and A L Owczarek

Department of Mathematics and Statistics, The University of Melbourne, Victoria 3010, Australia

E-mail: andrewr@ms.unimelb.edu.au and aleks@ms.unimelb.edu.au

Received 18 October 1999, in final form 2 February 2000

Abstract. In two dimensions the universality classes of self-avoiding walks (SAWs) on the square lattice, restricted by allowing only certain two-step configurations (TSCs) to occur within each walk, has been argued to be determined primarily by the symmetry of the set of allowed rules. In three dimensions early work tentatively found one (undirected) universality class different to that of unrestricted SAWs on the simple cubic lattice. This rule was a natural generalization of the square lattice 'spiral' SAW to three dimensions. In this report we examine a variety of three-dimensional SAW models with different step restrictions, carefully chosen so as to search for a connection between the symmetry of the rules and possible new universality classes. A first analysis of the scaling of the radius of gyration suggests several universality classes, including the one found earlier, and perhaps some novel class(es). However, a classification of these universality classes using the symmetries of the rules, or other basic rule properties, is not evident. Further analysis of the number of configurations and moment of inertia tensor suggests that in three dimensions the only non-trivial or undirected universality class is that of unrestricted SAWs.

1. Introduction

The self-avoiding walk (SAW) (see, for example, [1] and references therein) and its derivatives have been a major source of models describing the thermodynamic, geometric and topological properties of different types of long chain polymers in solution. A large number of modifications, such as the addition of various interactions (e.g. surface or intra-polymer) or particular restrictions (e.g. directedness), have been made to the basic model to mimic either various physical situations or to allow for easier analysis (such as exact solution). Some of these changes in the basic model modify the scaling behaviour of system properties, and hence change the universality class. For example, it is well known that restricting SAWs on the square or cubic lattices by only allowing steps in the positive axial directions, thus producing so-called directed (or rather fully directed) walks (see [2,3]), changes the way that the radius of gyration scales with polymer length. Geometric restrictions, such as directedness or spirality, are one particular type of modification whose effect on the scaling behaviour of walks is of considerable interest. Non-directed but restricted walks were first introduced by Grassberger [4] and the models he examined were found to be in the same universality class as SAWs. However, spiral SAWs (SSAWs) [5–8] on the square lattice were subsequently found to be in a different universality class to unrestricted SAWs (and, of course, directed walks (DWs)). Another novel universality class, studied subsequently [9–13], is that of anisotropic SSAWs (ASSAWs), also defined on the square lattice. This class has proven difficult to analyse [13] but appears to be distinct from the other classes.

0305-4470/00/142685+39$30.00

The SAW models previously analysed that give rise to the various universality classes of walks with geometric constraints can be described by the title 'two-step-restricted walks' (TSRWs) since these models are specified by the directions in which subsequent steps are allowed after steps in each of the four (square lattice) lattice directions are made. For example, one might specify that after either positive x- or y-axis steps only positive x- or y-axis steps can be made and that negative steps are disallowed—this gives the fully DW. Such rules might model oriented polymers in complicated external fields. We note here that these TSRW models are by their nature oriented. In two dimensions a wide-ranging study [12] of the universality classes, as determined by the scaling of the mean square end-to-end distance, of two-step-restricted SAWs on the square lattice, without interactions, has been made. Apart from cataloguing the universality classes in two dimensions, and analysing the ASSAW class further, this study elucidated the relationship between the symmetries of the lattice models and their universality classes. The study found that symmetry was a major factor in deciding into which universality class a rule's configurations would fall.

The theoretical understanding of the effect of geometric restrictions on the scaling behaviour of three-dimensional SAWs is less well understood. Guttmann and Wallace [14] introduced two walk models on the simple cubic lattice, which they called model S and model A. Model A was argued to be in the same universality class as three-dimensional SAWs, while the model S, a three-dimensional equivalent of the spiral walk, appeared to be a member of a distinct class.

In this work we examine a subset of the possible two-step restriction rule models on the simple cubic lattice in a manner similar to that of Guttmann *et al* [12]. Our purpose in doing this is twofold: firstly to determine the possible universality classes for such rules in three dimensions and secondly to attempt to find a similar relationship between the symmetry of the microscopic rule and the macroscopic scaling behaviour of the ensemble of walk configurations, as in the work of Guttmann *et al* [12]. We focus on rules that are likely to produce configurations that are not simply directed, or zero, one- or two-dimensional. Exact enumeration and subsequent series analysis has been the basis of our studies here. Our first analyses on the radius of gyration series show the possibility of novel universality classes in three dimensions. However, no correspondence can be made between the symmetry of the rules and these apparent universality classes. Also, the difference in the exponents between different universality classes is relatively small. More detailed analysis paints a different picture: that there are no 'real' equivalents of the spiral or anisotropic spiral classes among three-dimensional two-step rules—that is, there are no novel universality classes—and so we deduce that the unique topology of two dimensions must be an important factor in determining the number of different universality classes there.

We begin our discussion in the next section with the definition of a TSRW model. The space of TSRW models is much larger in three dimensions than in two. To understand the factors important in our choice of models to study we first review the results of earlier square lattice studies with a view to extracting the salient features. We provide a complete pictorial classification of the interesting square lattice TSRW models in appendix A. This motivates the cubic lattice models we have studied, which we describe in section 2 also. We then describe the generation of our exact enumeration data and its various analyses in section 3. Finally, in section 4 we provide a discussion of our numerical results, summarizing the different reasonable theoretical scenarios, and cautiously pointing out the most likely conclusions.

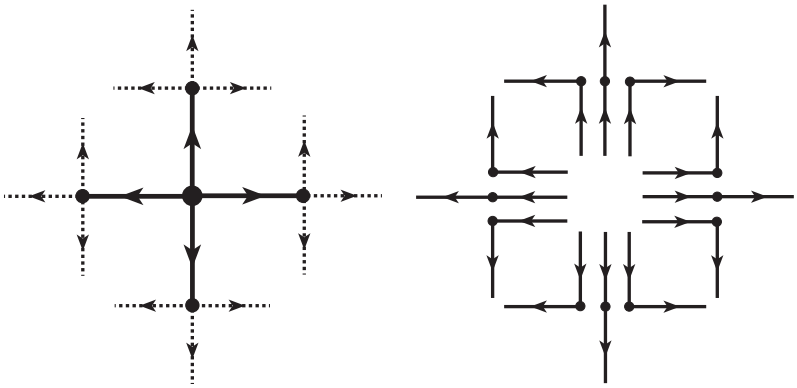

Figure 1. The construction of the allowed TSCs in a TSRW starts in (*a*) with the consideration of each of the possible bonds (full lines) of a vertex. One specifies which of the next steps (dashed lines) is allowed. Shown here also in (*b*) are the 12 square lattice TSCs.

2. Two-step-restricted walk models

2.1. Definition

In this paper we consider two-step-restricted SAW (TSRW) models on the square and simple cubic lattices. However, this type of model can be defined on any lattice with a finite number of types of vertices. To be specific, and for the sake of simplicity, let us first consider the square lattice problem. One begins by considering oriented SAWs on this lattice (starting from some fixed origin). To specify the model one does two things. The first is to generate a set of allowed two-step configurations. To do this one considers a vertex of the lattice and, in turn, each of the bonds emanating from that site. On the square lattice there are four bonds emanating from each site. Assuming a step of the walk is on the bond (one of the four) under consideration one then specifies the bonds that are allowed for the next step of the walk. From each of the four first-step bonds there are three possible continuing bonds (considering self-avoidance). This means there are 12 possible TSCs for an oriented SAW on the square lattice. Figure 1 illustrates this construction with the possible 12 TSCs explicitly given. To specify a TSRW model one must say which of the 12 two-step configurations are allowed and which are not allowed. There are hence $2^{12} = 4096$ possible rules, and so 4096 walk models. Figure 2 illustrates one TSRW rule with the associated allowed TSCs also shown. The second part in obtaining a model is to take all oriented SAWs on the lattice where each two-step segment of each walk is one of the allowed TSCs. One then can ignore the orientation and this leaves a set of SAWs which then defines a two-step-restricted rule model.

Now, as mentioned above, this construction can be made on any regular lattice. On a d-dimensional hypercubic lattice the cardinality of the rule space is $2^{2d(2d-1)}$, so while in two dimensions the cardinality of the rule space is $2^{12} = 4096$, in three dimensions it is $2^{30} = 1073\,741\,824$. The size of the three-dimensional rule space leads us first to re-examine the two-dimensional rule space more carefully.

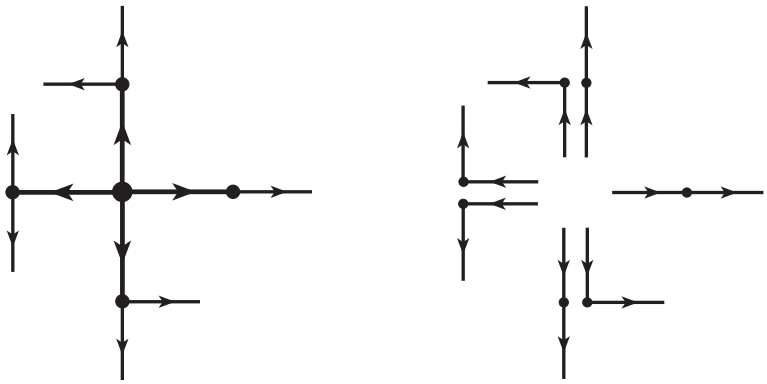

(*a*) (*b*)

Figure 2. A particular TSRW rule is illustrated in (*a*) with the associated allowed two-step configurations shown in (*b*).

2.2. Two dimensions

2.2.1. Summary of two-dimensional results. On the square lattice Guttmann *et al* [12] have catalogued the classes of two-step-restricted SAWs, and examined the relationship between the scaling of the size of the objects, as measured by the various components of the end-to-end distance, and the symmetries of the walk rule. Some SAW models on other two-dimensional lattices have also been considered previously. Most notably the unrestricted SAW on the triangular and honeycomb lattices [15–17] appear, within error calculations, to be in the same universality class as square lattice SAWs. Variants of the spiral SAWs on the triangular lattice have also been studied [18–20]. At least with respect to the scaling of the size of the walks, as measured by the radius of gyration for example, the triangular and square lattice SAWs show similar scaling behaviour.

In Guttmann *et al* [12] the universality class was delineated mainly by considering the mean square end-to-end distance $\langle R_e^2 \rangle_n$ scaling of these walk models with walk length n, this being a measure of the size of the model polymer similar in behaviour to the radius of gyration, $\langle R_g^2 \rangle_n$. The exponent associated with any measure of the average area of configurations, $\langle R^2 \rangle_n$, is denoted ν and one usually expects the dominant asymptotic form to be

$$\langle R^2 \rangle_n \sim A n^{2\nu} \qquad \text{as} \quad n \to \infty. \tag{2.1}$$

For SAWs without restriction in two dimensions it is expected that $\nu = \frac{3}{4}$ [21], regardless of lattice. To be most general one needs to define scaling exponents in the maximal and minimal scaling directions, that is $\nu_\parallel$ and $\nu_\perp$ respectively. The work of Guttmann *et al* [12] concluded that there are seven universality classes of two-step restriction models on the square lattice delineated by their 'size' scaling. Three of these are such that neither of the exponents take on the values 1 or 0 (these values imply some kind of one- or zero-dimensional behaviour respectively). These three classes are: unrestricted SAWs with $\nu_\parallel = \nu_\perp = \frac{3}{4}$; SSAWs where $\nu_\parallel = \nu_\perp = \frac{1}{2}$ [8, 18] with confluent multiplicative logarithmic factors in the asymptotic form; and ASSAWs where the latest Monte Carlo evidence [13] suggests $\nu_\parallel = 2\nu_\perp = 0.95(2)$. To be precise, the scaling form [8, 18] for SSAW geometric size has been derived exactly as

$$\langle R^2 \rangle_n \sim A_{Sp} n (\log n)^2 \qquad \text{as} \quad n \to \infty. \tag{2.2}$$

The ASSAW model has certainly been the hardest to characterize and this may also be because of the existence of confluent logarithms in the scaling form for $\langle R^2 \rangle_n$ for that class [13]. There

Table 1. The scaling of the number of configurations, c_n, for several two-dimensional walk models.

Walk model	Scaling form for the number of walks	Exponent and constant values or estimates
SAW	$c_n \sim B\mu^n n^{\gamma-1}$	$\gamma = \frac{43}{32}$ [21]
Square spiral	$c_n \sim B\mathrm{e}^{\frac{2\pi}{\sqrt{3}}\sqrt{n}} n^{\beta}$	$\beta = -\frac{7}{4}$ [5–8]
Triangular spiral I	$c_n \sim B\mathrm{e}^{\pi\sqrt{\frac{2}{3}}\sqrt{n}} n^{\beta}$	$\beta = -\frac{5}{4}$ [18]
Triangular spiral II and III	$c_n \sim B\mathrm{e}^{2\pi\sqrt{n}} \log\left(\frac{n}{12}\right) n^{\beta}$	$\beta = -\frac{13}{4}$ [20]
ASSAW	$c_n \sim B\mu^n \mathrm{e}^{a\sqrt{n}} n^{\beta}$	$\beta \approx 0.9$, $a \approx 0.14$ [11]
DW	$c_n \sim B\mu^n$	$\mu > 1$ and $\gamma = 1$ [22]

is no apparent exact solution for any ASSAW rule as there is for the SSAW class. A point worth noting here is that the radius of gyration seems to be affected by smaller corrections-to-scaling than the mean square end-to-end distance [13], and so exponent estimates obtained from the radius of gyration converge more quickly to a stable asymptotic value.

The classification of rules not falling into one of the three classes mentioned above is given by the following: some rules do not produce any long walks so $\nu_{\parallel} = 0$ and $\nu_{\perp} = 0$, that is, they are trivial or zero-dimensional rules; there are one-dimensional rules with $\nu_{\parallel} = 1$ and $\nu_{\perp} = 0$ where configurations are essentially made up of a single one-dimensional walk; there are rules that produce configurations made up of different one-dimensional walks, perhaps concatenated together a bounded number of times—they have $\nu_{\parallel} = 1$ and $\nu_{\perp} = 1$; finally, some rules give walks that fall into the universality class of DWs with $\nu_{\parallel} = 1$ and $\nu_{\perp} = \frac{1}{2}$ (these are often described as $(1+1)$-dimensional or even '$\frac{3}{2}$'-dimensional).

The other property that has been commonly used to classify the behaviour of a SAW model is the scaling, or asymptotic form, of the number of configurations (or partition function), c_n, of length n. For SAWs it is usually expected that the dominant asymptotic form of c_n is given by

$$c_n \sim B\mu^n n^{\gamma-1} \qquad \text{as} \quad n \to \infty \tag{2.3}$$

where μ is the 'connective' constant and γ is the universal entropic critical exponent. However, the scaling forms of c_n for SSAWs and ASSAWs have been shown, exactly in the case of SSAWs [5–8, 18], and predicted numerically in the case of ASSAWs [11], to have different forms. The two-dimensional results for c_n are summarized in the table 1. Only in the case of unrestricted SAWs and DWs is it possible to interpret the power of the algebraic factor as a critical exponent (only in these cases does the associated generating function have a dominant algebraic singularity). The models labelled triangular spiral II and III have a multiplicative logarithmic confluent factor in their scaling form relative to the square lattice spirals. The geometric size scaling for these models remains undetermined so it is unclear how to interpret the triangular lattice results. It is likely that the geometric size scaling is less sensitive to minor variations in the model and that the exponent ν for these models is $\frac{1}{2}$ (log) as in the case of square lattice spiral and 'triangular spiral I' walks.

2.2.2. Discussion of square lattice rules. We now concentrate on the classification of the square lattice TSRW models via their geometric scaling form. As described above, Guttmann *et al* [12] found that there are seven universality classes. They also attempted to ascertain the microscopic constraints on the rules that determine the geometric scaling form of the walks. They concluded that three factors were important in determining the universality class. The first

Table 2. Length scale exponents and symmetries for the seven known two-dimensional universality classes of two-step-restricted rule SAW. We define a one letter code for each class. The letter 'y' stands for 'yes', 'n' for 'no', and 'e' for 'either'.

Rule	$\nu_\parallel$	$\nu_\perp$	Rotation by 90°	Rotation by 180°	Reflection
SAW (S)	$\frac{3}{4}$	$\frac{3}{4}$	e	y	y
Spiral (P)	$\frac{1}{2}$(log)	$\frac{1}{2}$(log)	y	y	n
Anisotropic spiral (A)	0.95(2)	0.47(1)	n	y	n
Directed (D)	1	$\frac{1}{2}$	n	e	e
Pseudo-1D (U)	1	1	e	e	e
1D (O)	1	0	n	e	e
Trivial (T)	0	0	e	e	e

was the (somewhat imprecise) idea that there must be enough of the 12 TSCs allowed to give a non-trivial or non-one-dimensional rule. Secondly, they quoted 'balance' as a criterion: rules that do not have equal numbers of continuing steps in the positive and negative components of each axis are either directed, one-dimensional or trivial. This criterion was tested for several rules and seems to be well borne out by the exact enumeration studies. One can also argue that if the rule is unbalanced then the random walk generated with the rule will be directed. Furthermore, one can plausibly conjecture that adding self-avoidance should not affect this directedness. Hence, unbalancedness is a good indication that the SAW generated with this rule is directed also. Note, however, that the converse is not true: the 'balance' condition is satisfied by some rules that give directed and one-dimensional walks. The final determining factor in the classification of the non-directed and non-one-dimensional (and trivial) rules was argued to be that of symmetry. The symmetries involved are single rotations and reflections: on the square lattice rotations by π and $\frac{\pi}{2}$, and reflections about the lines $\theta = 0, \frac{\pi}{4}, \frac{\pi}{2}, \frac{3\pi}{4}$. In table 2 the seven (geometric scaling) universality classes are listed, along with the symmetries obeyed by the various rules in that class. So if one excludes directed, one- or zero-dimensional TSRW rules then:

- All SAW-like rules have rotation-by-π symmetry and some reflection symmetry.
- All spiral-like rules have rotation-by-$\frac{\pi}{2}$ (and hence rotation-by-π) symmetry but no reflection symmetry.
- All ASSAW-like rules have rotation-by-π symmetry but no rotation-by-$\frac{\pi}{2}$ or reflection symmetries.

To be able to tackle the three-dimensional TSRW models let us first consider this classification in a little more depth. The balance condition can be expanded. Since one can always obtain the same walk configurations of a particular rule by considering the 'reverse' rule, which is obtained by reversing the orientation on the set of TSCs (and reversing the origin of the walks), it is sensible to also enforce a balance condition on the reversed walk of any rule one requires to be non-directed or non-one-dimensional. We denote this the 'reverse-balance' condition. Note that there are rules that are balanced but not reverse-balanced and so produce such walks in the directed or one-dimensional universality classes (see, for example, rule (k) in [12]). As mentioned previously, there are 4096 TSRW models on the square lattice. There are, however, only 80 such rules that obey the balance and reverse-balance conditions, which we shall refer to as the *symmetric-balance* condition from now on. For completeness we provide a complete catalogue of the 80 two-dimensional symmetric-balanced rules in appendix A, with classification according to the total number of continuing steps and universality class. The symmetries mentioned above mean that there are in fact only 24 distinct symmetric-balanced

rules on the square lattice. ÔDistinct rulesÕ here implies that the set of walk configurations are distinct up to lattice symmetries.

However, there is clearly one further criterion missing to distinguish the 'interesting' rules. One can see in hindsight that none of the rules that are symmetric-balanced and fall into the D, U, O or T classes obey the following condition: that from each of the four directions one can by a sequence of allowed steps end up in any direction (including itself again) while obeying self-avoidance. We call this the *mixing* condition: it is, of course, related to the fact that there are 'enough' continuing steps in each direction.

So, following on from Guttmann *et al* [12] one can write down a simple set of rules to determine if a rule produces walks in one of the S, P or A classes. Starting with all TSRW rules:

(1) All rules that are not symmetric-balanced are directed, one-dimensional or trivial (that is in the D, U, O or T classes).
(2) All symmetric-balanced rules that are not 'mixing' rules are also in the D, U, O or T classes.
(3) All symmetric-balanced and mixing rules that have reflection symmetry about any axis are of the SAW (S) universality class (expect possibly one rule which we call the anti-spiral model—see appendix A).
(4) All symmetric-balanced and mixing rules that do not have a reflection symmetry but are symmetric with respect to a rotation by $\frac{\pi}{2}$ are in the SSAW (P) universality class.
(5) All symmetric-balanced and mixing rules that are neither reflection symmetric nor symmetric under a $\frac{\pi}{2}$ rotation are in the ASSAW (A) class.

Note that all rules in the S, P and A classes (in fact, of the original 4096 there are only 22 rules—seven distinct rules—in these classes) with the exception of the rule mentioned in the appendix, called the anti-spiral, are symmetric with respect to rotations of π. (If the anti-spiral was in a novel universality class then the above classification would simply be expanded to distinguish the symmetric-balanced and mixing rules that have a reflection symmetry but no rotation symmetry at all.)

It is also interesting to note that one can distinguish the non-one-dimensional and non-DW by examination of their turning numbers. We define the turning number for a two-dimensional walk rule as the square of the difference of the number of TSCs that make a left turn to the number of TSCs that make a right turn. Those TSCs that proceed straight ahead make no contribution to the turning number. Using the turning number we could replace the last three steps in the above classification scheme by:

(3) (S) rule walks have turning number 0,
(4) (P) rule walks have turning number 16 and
(5) (A) rule walks have turning number 4.

The anti-spiral has turning number 0.

So, in summary, the set of TSRW rules giving walks in the 'interesting' classes of S, P and A are distinguished from other rules by the symmetric-balance and mixing conditions, while they are distinguished from each other by the consideration of the symmetry of the rules. We note that it may be possible to distinguish rules in the D, U, O or T classes from each other but this is of less interest.

2.3. Three dimensions: delineating properties of the two-step rule space

In two dimensions the cardinality of the TSRW rule space is $2^{12} = 4096$, while in three dimensions it is $2^{30} = 1073\,741\,824$. In this paper we shall follow the lessons learned in

the discussion of two-dimensional models described above. We do this by only considering rules that are symmetric-balanced and mixing. Let us call the set of TSRW rules that obey the symmetric-balanced and mixing conditions the symmetric-mixing rules. So let us consider the implications of these conditions for the space of three-dimensional TSRW rules.

2.3.1. Characterizing symmetric-balanced rules. On the simple cubic lattice there are 30 two-step configurations, so we could encode a particular rule by a 30 bit binary number. Alternatively we can encode the rules using a 6×6 square matrix of zeros and ones in the following way (six because vertices are sixfold coordinated on the simple cubic lattice). We label the lattice axes in the usual way with x, y and z, and steps in the $\pm x$ as $\boldsymbol{r}$ and $\boldsymbol{l}$ respectively, steps in the $\pm y$ as $\boldsymbol{f}$ and $\boldsymbol{b}$ respectively, and steps in the $\pm z$ as $\boldsymbol{u}$ and $\boldsymbol{d}$ respectively. Hence a TSC made up of an 'up' step in the positive z direction followed by a 'backward' step in the negative y direction is labelled as $\boldsymbol{ub}$. We define the matrix, $\boldsymbol{M}$, as

$$\boldsymbol{M} = \begin{bmatrix} \boldsymbol{rr} & 0 & \boldsymbol{rf} & \boldsymbol{rb} & \boldsymbol{ru} & \boldsymbol{rd} \\ 0 & \boldsymbol{ll} & \boldsymbol{lf} & \boldsymbol{lb} & \boldsymbol{lu} & \boldsymbol{ld} \\ \boldsymbol{fr} & \boldsymbol{fl} & \boldsymbol{ff} & 0 & \boldsymbol{fu} & \boldsymbol{fd} \\ \boldsymbol{br} & \boldsymbol{bl} & 0 & \boldsymbol{bb} & \boldsymbol{bu} & \boldsymbol{bd} \\ \boldsymbol{ur} & \boldsymbol{ul} & \boldsymbol{uf} & \boldsymbol{ub} & \boldsymbol{uu} & 0 \\ \boldsymbol{dr} & \boldsymbol{dl} & \boldsymbol{df} & \boldsymbol{db} & 0 & \boldsymbol{dd} \end{bmatrix} \tag{2.4}$$

where the elements are 1 or 0 depending on whether the corresponding TSCs occur in the rule space or not, respectively. That is, if the TSC $\boldsymbol{ub}$ occurs in our rule then the position $(5, 4)$, labelled by $\boldsymbol{ub}$ in equation (2.4) above, will contain a 1, otherwise it contains 0. For general dimensional hypercubic lattices the matrix $\boldsymbol{M}$ has binary elements with fixed zero elements for positions $(2k-1, 2k)$ and $(2k, 2k-1)$ for all $k \in \{1, \ldots, d\}$.

We can write the various balance restrictions for the hypercubic lattice simply as follows: the balance condition requires that the sum of elements of $\boldsymbol{M}$ in successive columns taken in pairs is the same, that is

$$\sum_i \boldsymbol{M}_{i,(2k-1)} = \sum_i \boldsymbol{M}_{i,2k} \qquad \text{for} \quad k \in \{1, \ldots, d\} \tag{2.5}$$

while the reverse-balance condition requires that the sum of elements of $\boldsymbol{M}$ in successive rows taken in pairs is the same, that is

$$\sum_j \boldsymbol{M}_{(2k-1),j} = \sum_j \boldsymbol{M}_{2k,j} \qquad \text{for} \quad k \in \{1, \ldots, d\}. \tag{2.6}$$

The number of such rules can be calculated, and further, the detailed numbers of such rules made from a fixed number of TSCs can be calculated (see appendix B) by constructing a generating function that sums over all allowed matrices $\boldsymbol{M}$ subject to the constraints (2.5) and (2.6) above. The above construction can be applied in any dimension and in appendix B we have calculated the total number of symmetric-balanced rules as

- 80 walk models in two dimensions,
- 432 096 walk models in three dimensions and
- 478 340 593 664 walk models in four dimensions.

This subset of symmetric-balanced two-step rules is manageable in two dimensions (we have in fact catalogued them completely in this paper). However, in three dimensions it is far too large to be examined in its entirety.

2.3.2. Symmetries of TSRW rules in three dimensions. By restricting the consideration to only distinct symmetric-balanced rules the number of rules on the square lattice falls from 80 to 24. If we further add mixing to the constraints imposed then this number falls to seven. So we now consider the symmetries of cubic lattice TSRW. This serves a dual purpose. The symmetries allow us to focus our attention on the distinct rules (rules that give distinct ensembles) and also provides a possible set of conditions that may be used to delineate any new universality classes discovered, as in two dimensions. We also consider the turning number as a property that may also delineate such classes.

We now list all single rotations and reflection symmetries of the rules, as well as defining what we call the turning number of the rule. We also define a symmetry we call flip-symmetry: this was considered since its existence is a quick way to ensure that the rule is symmetric-balanced. The properties we have used in three dimensions to attempt to classify TSRW rules are

(1) Rotational symmetries about the coordinate axes
   - $\pm\frac{\pi}{2}$
   - π.

(2) Reflection symmetries
   - reflection in coordinate planes. The normals of these planes are given by: $\vec{n} = \hat{e}_x$, $\hat{e}_y$, $\hat{e}_z$; the unit vectors in each axial direction.
   - reflection in diagonal planes†. The normals of these planes are given by: $\vec{n} = (\hat{e}_x \pm \hat{e}_y)$, $(\hat{e}_x \pm \hat{e}_z)$, $(\hat{e}_y \pm \hat{e}_z)$.

(3) Turning number
   - The turning number for a three-dimensional walk rule is the sum of the turning numbers of the planar walk rules in each co-ordinate plane when viewed from the positive side of the co-ordinate axis normal to that plane.

(4) Flip symmetry
   - send each co-ordinate to its negative. In two dimensions this is equivalent to rotation by π. If a walk has the flip symmetry, then it is balanced and reverse-balanced. The reverse is not true.

It should be noted that it can be easily shown that TSRW rules in three dimensions with a $\frac{\pi}{2}$ rotational symmetry have a plane of reflection; the normal of the plane of reflection is the axis of the rotation. The converse is not true.

So in later discussion we attempt to classify the rules studied into universality classes according to which *single* symmetry operations acting on the rules leave the rules unchanged. All the rules (bar one) examined had the flip symmetry, and as noted above this implies all the rules were symmetric-balanced.

2.4. Construction of symmetric-mixing cubic lattice TSRW rules

Without actually going through all 432 096, or even the smaller number of distinct iso-symmetric sets, of the symmetric-balanced TSRW rules on the cubic lattice we wanted to be

† The operator to reflect a vector in the plane with normal vector $\vec{n} = (\hat{e}_x + \hat{e}_y + \hat{e}_z)$, is given by the matrix:

$$R_{(\hat{e}_x+\hat{e}_y+\hat{e}_z)} = \tfrac{1}{3}\begin{bmatrix} 1 & -2 & -2 \\ -2 & 1 & -2 \\ -2 & -2 & 1 \end{bmatrix}.$$

From this matrix we see that the vector $\hat{e}_x$ is mapped to $\frac{1}{3}(\hat{e}_x - 2\hat{e}_y - 2\hat{e}_z)$. That is, this operator is not closed on the vector space $\mathbb{Z}^3$. Hence a walk rule cannot have symmetry under this reflection, nor reflections in planes with normals given by $(\hat{e}_x \pm \hat{e}_y \pm \hat{e}_z)$.

able to choose a set of three-dimensional rules that adequately explored this set of models (by encompassing the different symmetries, etc). We also wanted to ensure the mixing condition held. To do this we chose to consider walk rules in three dimensions such that on each of the three axial planes the rule was one of a small number of planar walks. We chose to construct rules using representatives from most of the two-dimensional universality classes. We chose from the following rules (see the catalogue of rules in appendix A for the rule numbers):

- S Rule 1—Unrestricted planar SAW: in class (S), turning number 0;
- 3 Rule 5—Three-choice walks: in class (A), turning number 4;
- 2 Rule 6(a)—Two-choice walks: in class $4(A)$, turning number 4;
- P Rule 1—Planar spiral walks: in class (P), turning number 16;
- D Rule 7—DW (with reverse): in class (D), turning number 0;
- C Rule 22—Walks that are concatenations of 1d walks: in class (U), turning number 0;
- O Rule 19—Walks that are one-dimensional along either axis: in class (U), turning number 0;
- R Rule 17—Walks that form incomplete one-dimensional rectangles: in class (O) turning number 4.

Each three-dimensional rule we considered can be given a three letter code such as $(P\text{-}O\text{-}3)$, which means the plane with a normal along the z-axis was given the square lattice rule (P) while the plane with a normal along the y-axis was given the square lattice rule (O) and the plane with a normal along the x-axis was given the square lattice rule (3). The three-dimensional SAW is denoted by $(S\text{-}S\text{-}S)$, Guttmann and Wallace's spiral walk [14] (model S) is $(P\text{-}P\text{-}P)$ while Guttmann and Wallace's 'anisotropic spiral' 3D-equivalent (model A) is $(S\text{-}C\text{-}3)$. Note that not every combination of these types is possible; for example, one cannot construct a $(S\text{-}3\text{-}2)$ walk. This is because each quadratic lattice walk is defined by 12 choices of TSCs that is made, and since there are three axial planes we have a total of 36 choices to make. However, in three dimensions one really has only 30 possible choices to make, so some combinations will be inconsistent (and so impossible). The five models that we have analysed most extensively are illustrated in figures 3–7. In figure 3 the rule $(P\text{-}P\text{-}P)$ is shown, in figure 4 the rule $(P\text{-}2\text{-}2)$ is shown, in figure 5 the rule $(P\text{-}O\text{-}3)$ is shown, in figure 6 the rule $(S\text{-}C\text{-}P)$ is shown, while in figure 7 the rule $(P\text{-}R\text{-}2)$ is shown. Note that the turning number of the three-dimensional rule is simply the sum of the turning numbers of the three two-dimensional rules that make up the rule.

In fact we have examined by exact enumeration studies all the walk rules constructed plane-by-plane with the added restriction of not having more than one plane with a one-dimensional or directed rule (D, C, O or R). This restriction was made to ensure we ended up with three-dimensional rules that were mixing. We considered the 38 such rules initially. All these rules had flip-symmetry and so were symmetric-balanced, and therefore symmetric-mixing. This was still too many rules to consider in depth and because of the larger connective constants in three dimensions than in two the series enumerated were relatively shorter. We chose the nine most promising rules from a numerical point of view that covered many of the symmetry combinations plus three other rules (one not constructed in the above manner) so as to include all possible symmetry combinations. These rules included both the rules considered by Guttmann and Wallace previously [14].

We especially constructed a rule outside the gamut of the procedure described above so as to produce a rule that was symmetric under rotations by π but not under rotations by $\frac{\pi}{2}$ or any reflection. We call this rule Rot-π and it is a symmetric-balanced rule. The M matrix for

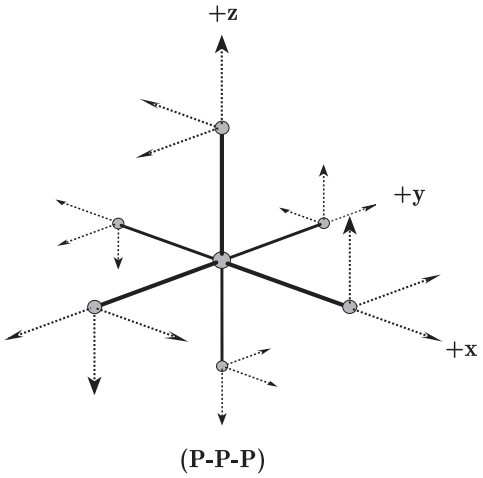

Figure 3. An illustration of the (*P*-*P*-*P*) rule.

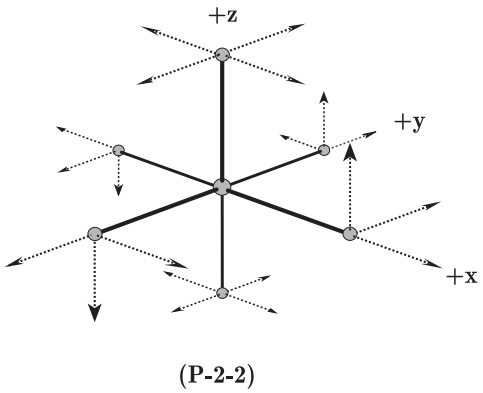

Figure 4. An illustration of the (*P*-2-2)rule.

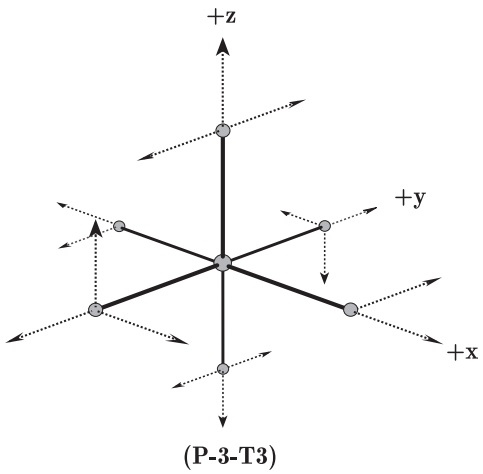

Figure 5. An illustration of the (*P*-*O*-3) rule.

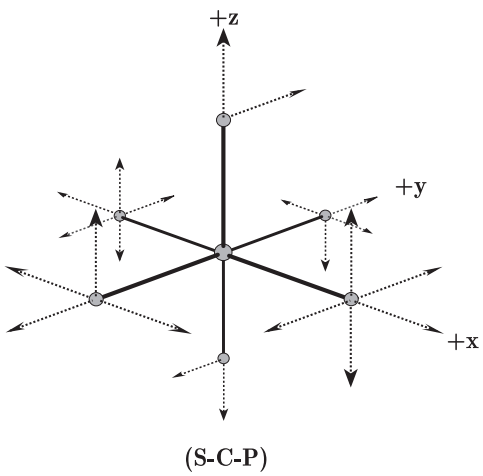

Figure 6. An illustration of the (*S*-*C*-*P*) rule.

this rule is

$$M_{\text{Rot-}\pi} = \begin{bmatrix} 1 & 0 & 1 & 0 & 1 & 0 \\ 0 & 1 & 0 & 1 & 0 & 1 \\ 0 & 1 & 1 & 0 & 0 & 1 \\ 1 & 0 & 0 & 1 & 1 & 0 \\ 0 & 0 & 1 & 1 & 1 & 0 \\ 1 & 1 & 0 & 0 & 0 & 1 \end{bmatrix}. \tag{2.7}$$

3. Exact enumeration results and analysis

We now describe the enumeration and analyses of the 11 TSRW models constructed plane-by-plane, in the manner described in the section 2.4. The rules were (3-3-*C*), (*S*-*C*-3), (*P*-2-2), (*P*-*R*-2), (*P*-3-3), (*P*-*O*-3), (*P*-*P*-*P*), (*S*-*P*-3), (*P*-*P*-3), (*P*-*P*-*D*) and (*S*-*C*-*P*). These were

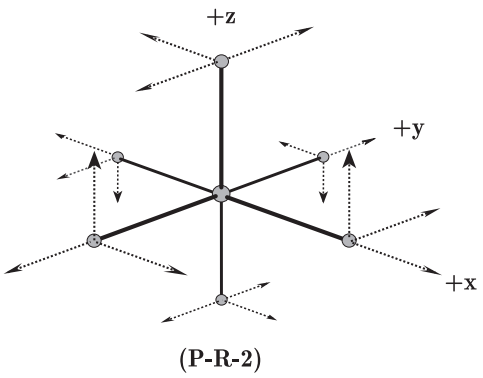

Figure 7. An illustration of the $(P\text{-}R\text{-}2)$ rule.

chosen from the original 38 models on which we performed short enumerations, not detailed here. We also considered the (Rot-π) rule, described above, to ensure the different possible symmetry combinations are covered. After the analysis of the 12 models we concentrated on the five models that were numerically best behaved and representative of the numerical behaviour found in the 12 models.

We began by enumerating the numbers of walks, c_n, and the total radius of gyration, r_n, where $\langle R_g^2 \rangle_n = r_n/c_n$, for each of the 12 models listed above using a recursive back-tracking algorithm up to various maximum lengths, $n \leqslant N$, that depended on the model. (Later we also calculated the full moment of inertia for five of the models.) We chose to calculate and analyse the radius of gyration rather than the end-to-end distance since in two-dimensional studies the asymptotic analysis of the radius of gyration [13] has proven less affected by corrections-to-scaling, as discussed in section 2. The lengths of the enumerations depended on the effective connective constants of the models, and our enumerations ranged in length, N, from 18 to 29. The initial enumerations of the 12 models are given in appendix C. In particular, we have increased the length of the enumerations for the $(P\text{-}P\text{-}P)$ model from 23 [14] to 29 and the $(S\text{-}C\text{-}3)$ model from 18 [14] to 23 steps. As an example, the $(P\text{-}P\text{-}P)$ enumerations up to length 28 took approximately 150 CPU hours on a Digital Alphastation 500/266.

3.1. Review of previous three-dimensional work

Unrestricted SAWs, $(S\text{-}S\text{-}S)$, on the cubic lattice have been studied by both exact enumeration [16] and Monte Carlo techniques [23, 24]. For unrestricted SAWs scaling theory [1] predicts that the number of walks scales as

$$c_n \sim B\mu^n n^{\gamma-1} \qquad \text{as} \quad n \to \infty \tag{3.1}$$

so

$$\sum_{n=0}^{\infty} c_n x^n \sim B'(1-\mu x)^{-\gamma} \qquad \text{as} \quad x \to \frac{1}{\mu^-} \tag{3.2}$$

and that the total radius of gyration scales as

$$r_n \sim D\mu^n n^{2\nu+\gamma-1} \qquad \text{as} \quad n \to \infty \tag{3.3}$$

so

$$\sum_{n=0}^{\infty} r_n x^n \sim D'(1-\mu x)^{-(2\nu+\gamma)} \qquad \text{as} \quad x \to \frac{1}{\mu^-} \tag{3.4}$$

while the average radius of gyration scales as

$$\langle R_g^2 \rangle_n \sim A n^{2\nu} \qquad \text{as} \quad n \to \infty \tag{3.5}$$

so

$$\sum_{n=0}^{\infty} \langle R_g^2 \rangle_n x^n \sim A'(1-x)^{-(2\nu+1)} \qquad \text{as} \quad x \to 1^-. \tag{3.6}$$

An exact enumeration study [16] on the simple cubic lattice, of SAWs up to length 21 found

$$\frac{1}{\mu} = 0.213\,496(4) \tag{3.7}$$

$$\gamma = 1.161(1) \tag{3.8}$$

and

$$2\nu = 1.184(8). \tag{3.9}$$

Various high-precision Monte Carlo studies using walks up to lengths $N = 40\,000$ and $N = 80\,000$ respectively have found $\gamma = 1.1575(6)$ [24] and $2\nu = 1.1754(12)$ [23]. To make a fair comparison with our series analysis of the 12 TSRW we shall only use the exact enumeration results quoted above for the unrestricted SAW model.

Guttmann and Wallace [14] studied both the (P-P-P) and (S-C-3) model by exact enumeration, with walk lengths up to 23 and 18 respectively. They calculated the end-to-end distance rather than the radius of gyration. They used a differential approximant analysis, and also various ratio analyses to study the models. The differential approximant analysis concluded that for the (P-P-P) model

$$\frac{1}{\mu} = 0.3765(2) \tag{3.10}$$

$$\gamma = 1.24(20) \tag{3.11}$$

and

$$2\nu = 1.3(4) \tag{3.12}$$

while for the (S-C-3) model

$$\frac{1}{\mu} = 0.2883(2) \tag{3.13}$$

$$\gamma = 1.16(2) \tag{3.14}$$

and

$$2\nu = 1.19(5). \tag{3.15}$$

The ratio methods gave more precise answers for the geometric-size exponents, $2\nu = 1.29(3)$ for the (P-P-P) model, and $2\nu = 1.18(1)$ for the (S-C-3) model. Note that, despite having similar numbers of terms as the unrestricted SAW enumeration, the analyses for these models give far less precise exponent estimates, and the series are far less well behaved under differential approximant analysis. Despite the large error bars on the differential approximant analyses, the further analyses via the ratio method led the authors to conjecture that the (S-C-3) model is a member of the unrestricted SAW universality class while the (P-P-P) model is part of a novel class, being a three-dimensional counterpart to the 2D-spiral class (P). They noted that both (S-C-3) rule and unrestricted SAWs have a plane of reflection symmetry while the (P-P-P) rule does not. They then concluded that this may be the microscopic criterion for the difference in the universality class, as it is in two dimensions. We note in passing that, while (S-C-3) possesses a rotation-by-π symmetry, the (P-P-P) rule has no rotation symmetry (in contradiction to the claim made in [14]), so that could equally well be the microscopic criterion.

3.2. Differential approximant analysis of c_n and $\langle R_g^2\rangle_n$ for 12 TSRW models

We first performed differential approximant analyses [25] on the number of walks, c_n and the radius of gyration $\langle R_g^2\rangle_n$ for the 12 TSRW models. We used second-order inhomogeneous approximants that utilized all the available coefficients, and we varied the range of the order of the polynomials to suit the lengths of the series. We checked some of the analyses with first- and third-order approximants. In general, the first-order approximants were not as well behaved and the third-order approximants gave similar results to the second-order approximants, though they could not be used effectively due to the short length of many of the series.

Since we had no *a priori* estimates for the critical points of the various c_n series, we arrived at our $\frac{1}{\mu}$ and γ estimates by using unbiased approximants, and obtained error estimates from the spread (standard deviations) of the approximants. The estimates calculated were the mean values and the errors were two standard deviations.

We then considered the radius of gyration series, $\langle R_g^2\rangle_n$. Since the generating function of $\langle R_g^2\rangle_n$ should have a critical point equal to unity we used this as one measure of the convergence of that series. Many of the $\langle R_g^2\rangle_n$ series were poorly converged compared with the unrestricted SAW series. Most also had a relatively wide spread of approximants. We found that using 'biased approximants', as per [25], yielded very poor results. Instead we arrived at a biased exponent estimate from the unbiased approximants in the following way: we took a large range of (unbiased) approximants, made a linear fit on the central section of the approximants and then extrapolated back to a critical point of $x = 1$. The various estimates and associated errors we calculated were taken from this linear fit. Firstly, we calculated the mean critical point and exponent of the approximants on which the linear fit was taken, which we denote $\bar{x}_c$ and $2\bar{\nu}$ respectively (errors are two standard deviations). Secondly, we calculated the estimate from linear biasing itself, $2\nu_{\mathrm{LB}}$ (error quoted is the error from the linear regression). The final estimate, $2\nu_{\mathrm{final}}(\Delta_{\mathrm{stat}})(\Delta_{\mathrm{sys}})$ is the same as the biased value, $2\nu_{\mathrm{LB}}$, but quoted with two errors: Δ_{stat} is the statistical error from the linear regression; while Δ_{sys} is a measure of the systematic error in biasing the approximants back to unity—it is equal to the difference between the mean exponent value and biased value, $|2\nu_{\mathrm{LB}} - 2\bar{\nu}|$. Using Δ_{sys} for our estimate of systematic error may be considered rather conservative, but this estimate has proved to be a useful measure of systematic error in other SAW problems, such as polymer adsorption [26]. A typical differential approximant spread for the $\langle R_g^2\rangle_n$ series is shown in figure 8, with illustrations of the various estimates and associated errors we calculated given.

The results from the differential approximant analysis are given in table 3. Considering the entropic exponent γ estimates in table 3, we find that the SAW value of 1.161 falls within the respective errors estimated for all the models. This would suggest one reasonable conclusion to be that all the models are in the *same* universality class as unrestricted SAWs. The $\langle R_g^2\rangle_n$ approximants, by contrast, seem to indicate that the models fall into possibly three different universality classes:

- SAW-*like*: (S-S-S), (S-C-3), (S-C-P), (3-3-C), (Rot-π) and (S-P-3);
- New: (P-3-3), (P-O-3) and (P-2-2);
- 3D-spiral: (P-P-P) and (P-R-2).

We were unable to classify the (P-P-3) rule because of the size of the associated error bars on the exponent estimates; however, it seems to lie in either the apparent 3D-spiral class or the new class, though it may, of course, form another class again. Though the results from the analysis of the data are too poor to draw any reasonable conclusions we have included the (P-P-D) data because of the symmetries of the walk rule and its winding number.

The spread of $\langle R_g^2\rangle_n$ approximants for several representative rules is shown in figure 9. This figure clearly shows what appears to be three separate bands of approximants representing

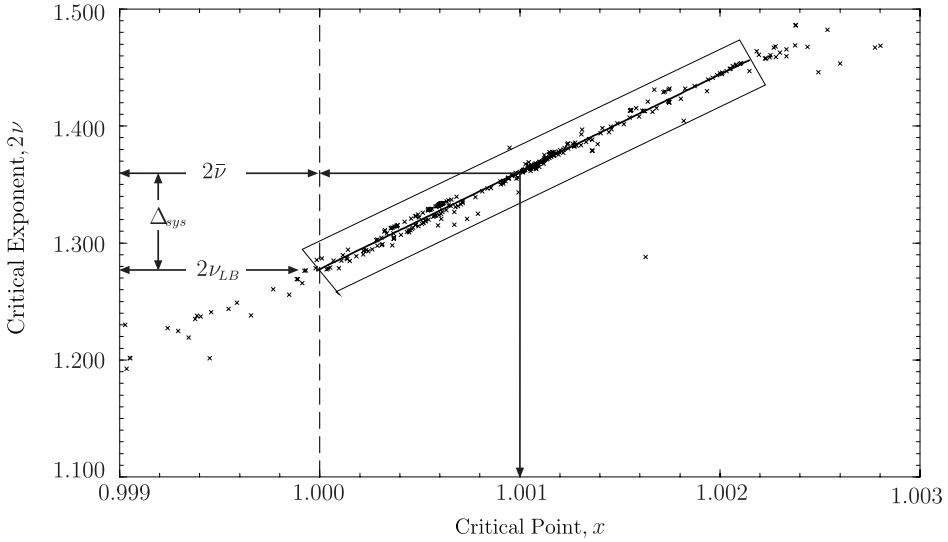

Figure 8. The differential approximant spread for the radius of gyration exponent, 2ν, for the (P-P-P) model. The box indicates the area over which an average was taken. A linear fit is shown which gives our 'biased' estimate, $2\nu_{\rm LB}$, from the point where the fit has an intercept with the dashed $x = 1$ vertical line. The arrows indicate the means of the boxed region's critical point, $\bar{x}_c$, and exponent, $2\bar{\nu}$. The difference between the boxed mean, $2\bar{\nu}$, and the biased estimate, $2\nu_{\rm LB}$, of the critical exponent gives us an estimate of systematic error, $\Delta_{\rm sys}$: in other walk problems this has usually proved to be conservative, though not always.

Table 3. Exponent estimates from differential approximant analysis. There are two sets of results for the (P-P-P) model, corresponding to second order and third order approximants. We include, for completeness, two sets of SAW (S-S-S) values, both obtained from exact enumeration data, one using our analysis method and one quoted from previous work.

Rule	$1/\mu$	γ	$\bar{x}_c$	$2\bar{\nu}$	$2\nu_{\rm LB}$	$2\nu_{\rm final}$
(S-C-3)	0.288 4(1)	1.16(2)	1.0002(4)	1.20(2)	1.19(1)	1.19(1)(1)
(3-3-C)	0.290 4(2)	1.16(2)	1.0005(6)	1.22(3)	1.19(1)	1.19(1)(3)
(S-P-C)	0.304 6(2)	1.17(2)	1.0002(7)	1.21(3)	1.20(1)	1.20(1)(1)
(S-P-3)	0.269 85(4)	1.169(6)	1.0003(3)	1.22(2)	1.21(1)	1.21(1)(1)
(Rot-π)	0.357 5(4)	1.17(4)	0.9997(14)	1.19(7)	1.20(1)	1.20(1)(1)
(P-3-O)	0.407 8(2)	1.18(3)	0.9999(4)	1.22(2)	1.226(6)	1.23(1)(1)
(P-3-3)	0.305 58(8)	1.173(14)	1.0002(2)	1.23(1)	1.220(5)	1.22(1)(1)
(P-2-2)	0.344 2(1)	1.18(1)	1.0003(3)	1.25(2)	1.23(1)	1.23(1)(2)
(P-P-3)	0.331 67(7)	1.176(8)	1.0008(2)	1.30(2)	1.25(2)	1.25(2)(5)
(P-P-D)	0.358 6(4)	1.17(4)	1.004(2)	1.50(8)	1.33(11)	1.33(11)(17)
(P-2-R)	0.373 9(2)	1.19(2)	1.0011(6)	1.36(3)	1.30(2)	1.30(2)(6)
(P-P-P) 2nd	0.375 7(1)	1.18(2)	1.001(1)	1.37(6)	1.29(2)	1.29(2)(8)
(P-P-P) 3rd	0.375 7(1)	1.17(4)	1.001(1)	1.36(10)	1.27(2)	1.27(2)(9)
SAW-here	0.213 497(10)	1.162(2)	1.0002(2)	1.20(1)	1.192(5)	1.19(1)(1)
SAW-there	0.213 496(4)	1.161(2)	—	—	—	1.184(6)

three separate universality classes. Our results in this section generally concur with those of Guttmann and Wallace [14] for the (S-C-3) and (P-P-P) models. On the other hand, it is difficult to be confident in the conclusions of these results due to the relatively large systematic errors in the ν estimates that arise from the biasing procedure. It is possible that the conclusion

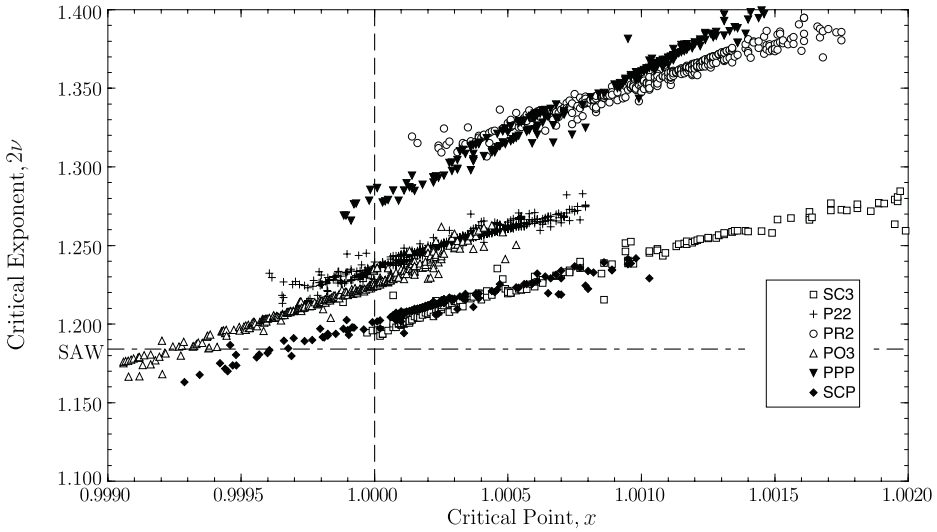

Figure 9. A plot of $\langle R_g^2 \rangle_n$ differential approximants for the exponent 2ν for several representative models. Notice the three distinct bands of approximants, each one made up from the approximants for several models. These bands seem to indicate that there are three universality classes.

that there is more than one universality class is a manifestation of corrections-to-scaling: the series being too short for the method of differential approximants to work effectively.

Assuming for the moment that the conclusions of the $\langle R_g^2 \rangle_n$ analysis are true, our next task was to attempt to establish the microscopic criteria that classify rules according to these apparent universality classes. We attempted this using the criteria that have proved useful in two dimensions. Given that all the rules are symmetric-balanced the various rule symmetries and the turning numbers were the candidates considered. The symmetries and turning numbers of these rules along with the maximum exact enumeration lengths are shown in table 4. All rules except (Rot-π) were flip symmetric. Note that the unrestricted SAW model, (S-S-S), has all the symmetries listed in table 4. Also, any rule that is symmetric under rotations by $\frac{\pi}{2}$ must be symmetric under rotations by π and also, as mentioned in section 2.3.2, must possess a reflection symmetry. Hence, the unrestricted SAW rule (S-S-S) is such a rule.

One can see immediately that all the rules in the new class, in the 3D-spiral class, and some in the SAW-like class do not have any rotation or reflection symmetries. Hence, these symmetries cannot be used to classify models into the apparent classes. In particular, reflection symmetry does not delineate the SAW class from the others. Hence, a classification according to symmetries of the rules is not forthcoming. A classification according to turning number would seem to be more successful (increasing turning number giving new classes at particular values, 20 and 36 perhaps). Here also there are problems: both the (S-P-3) and (P-O-3) rules have turning number 20 but seem to be in different universality classes and it is unclear in which class the model (P-P-3) lies despite having the same turning number as the model (P-R-2). These difficulties with an attempted microscopic classification and the consistency of the values of γ with the SAW value across all the rule models led us to examine the scaling behaviour of the models both using different quantities and with different analysis techniques in an attempt to find a consistent answer to this conflicting information.

We chose to examine five models representative of the apparent universality classes: (P-P-P) and (P-R-2) for the 3D-spiral class, (P-2-2) and (P-O-3) for the new class, and (S-C-P)

Table 4. Symmetries of the TSRW models examined. They are grouped according to the initial classification made from differential approximant analysis of the exact enumerations of the radius of gyration. The maximum length of the enumerations N is also given.

Class	Rule	N	Rotation by $\frac{\pi}{2}$	Rotation Rot-π	Any reflection	Turning number
SAW-*like*	(S-S-S)	21	y	y	y	0
	(S-C-3)	23	n	y	y	4
	(3-3-C)	20	n	n	n	8
	(S-C-P)	22	n	y	y	16
	(Rot-π)	22	n	y	n	16
	(S-P-3)	18	n	n	n	20
New	(P-O-3)	28	n	n	n	20
	(P-3-3)	24	n	n	n	24
	(P-2-2)	24	n	n	n	24
Undetermined	(P-P-D)	22	n	n	y	32
	(P-P-3)	25	n	n	n	36
3D-spiral	(P-R-2)	26	n	n	n	36
	(P-P-P)	29	n	n	n	48

representing the SAW class. We first considered further analysis of the c_n series that attempted to take account of non-standard scaling forms such as occurs in the two-dimensional spiral class (P), and secondly we analysed the mean moment of inertia tensor, $\langle \boldsymbol{I} \rangle_n$, to search for exponent anisotropy as occurs in the two-dimensional anisotropic spiral class (A).

3.3. Further analysis of c_n for five TSRW models

As stated above, we first expected that the number of walks, c_n, behaved according to equation (3.1) for each of the rule models: the differential approximant analysis described above fits to this form (with implicit corrections). However, different scaling forms have been found in some two-dimensional walk models. Two-dimensional spiral walks [5] and walks of the ASSAW class [11] have scaling forms that include $e^{\sqrt{n}}$ factors (see table 1). This additional factor present in the spiral walks' partition function scaling is mathematically related to the scaling of partitions of integers [5]; in three dimensions it may be possible that there will be plane-partition-like terms which scale as [27, 28]

$$p_n \sim C n^{-25/36} e^{a_{PP} n^{2/3}} \qquad \text{as} \quad n \to \infty. \tag{3.16}$$

We examined the possibility of corrections to the scaling form of the sort found in two-dimensional spirals and also those found in plane partitions. Differential approximant analysis (at least without significant modification) is unsuited to the study of such scaling forms, since the new factors imply that the generating function has an essential singularity. Of course, if such factors are present then the previous differential approximant analysis would have been inappropriate. With this in mind we attempted to make a direct fit of the data to the following forms:

$$c_n \sim C \mu^n n^{\gamma-1} \qquad \text{as} \quad n \to \infty \tag{3.17}$$

$$c_n \sim C \mu^n n^{\gamma-1} \exp(\alpha \sqrt{n}) \qquad \text{as} \quad n \to \infty \tag{3.18}$$

and

$$c_n \sim C \mu^n n^{\gamma-1} \exp(\alpha n^{2/3}) \qquad \text{as} \quad n \to \infty. \tag{3.19}$$

More precisely, we made successive fits using the series terms n, $n-2$, $n-4$ and $n-6$, as necessary, to each of the forms (which (linearly) contain 3 or 4 constants to ascertain)

$$\log c_n = a_1 + n\log\mu + (\gamma - 1)\log n \tag{3.20}$$

$$\log c_n = a_1 + n\log\mu + (\gamma - 1)\log n + a_2\sqrt{n} \tag{3.21}$$

and

$$\log c_n = a_1 + n\log\mu + (\gamma - 1)\log n + a_2 n^{2/3} \tag{3.22}$$

exactly. We made these fits with either γ free, or fixed at the SAW value (in the second case we used one less term at each stage). We did not attempt to consider multiplicative logarithmic corrections, as well as those above, since such forms are too difficult to fit with all but the longest series. The type of analysis described above is more refined than ratio analysis and has been used to great effect in SAW problems when considering corrections-to-scaling [29].

We illustrate the results of this fitting procedure in detail for the (P-P-P) walks in appendix D.2. To summarize, after examining tables D1 and D2, one can see that if corrections of the form $e^{\sqrt{n}}$ or $e^{n^{2/3}}$ are introduced, then they have coefficients very close to zero. This implies that any effect of these terms is quite negligible, and indeed that they are probably not present. We have found similar results for the other four walk models considered. This gives us confidence that the differential approximant analysis of c_n is giving reliable information. Hence, given that $e^{\sqrt{n}}$ or $e^{n^{2/3}}$ corrections seem not to be present in the scaling form for c_n, our original conclusion from the differential approximant analysis then stands: namely, that all the rules, including (S-S-S), have the same value of the γ exponent within error, being that of the SAW universality class (around 1.16). If the walks scale with subtly different exponents or multiplicative logs, the series at hand are too short to allow an investigation of these possibilities.

3.4. Analysis of the inertia tensor for five TSRW models

In our initial enumerations of the 12 models (as well as our very initial enumerations—not described here—of the 38 models of section 2.4) we enumerated the radius of gyration so as to measure the scaling of the average size of walks in the various models. To gain a finer view of the scaling of the geometric size we calculated the full moment of inertia tensor for the five models we designated for more intense study. This allowed us to look for any scaling anisotropy and to consider the eigenvalues of this matrix in addition to the radius of gyration.

The eigenvectors of the moment of inertia matrix correspond to the *natural* coordinate axes in which the ('average') walks scale, and the eigenvalues to the radius of gyration in those directions. For example, in two dimensions the three-choice walk model [12] has a mean moment of inertia tensor with eigenvectors $\{[1, 1], [1, -1]\}$, which correspond to the preferred and transverse directions. The eigenvalues for any three-dimensional TSRW model's moment of inertia matrix are expected to scale as

$$\lambda_j(n) \sim A_j n^{2\nu_j} \qquad j = 1, 2, 3 \qquad \text{as} \quad n \to \infty \tag{3.23}$$

where the values of ν_j and A_j may or may not be independent of direction j. Hence, there are two types of anisotropy: scaling anisotropy where different eigenvalues scale with different exponents ($\nu_i \neq \nu_j$), and a milder anisotropy where only the constants A_j differ. The moment of inertia tensor, $\boldsymbol{I}$, for a walk configuration φ_n of n steps, defined by the positions of its $n+1$ monomers (sites) as the set $\{\vec{r}_i = (x_i, y_i, z_i);\, i = 0, \ldots, n\}$, is given by

$$\boldsymbol{I}(\varphi_n) = \frac{1}{n+1}\sum_{i=0}^{n}(r_i^2\mathbf{1} - \vec{r}_i\vec{r}_i) \tag{3.24}$$

Table 5. Estimates of 2ν from the differential approximant analysis of the eigenvalues of the mean moment of inertia tensor computed about the centre of mass. Estimates of the critical points x_i of the associated generating functions are included to show quality of convergence. (P-P-P) has two eigenvalues, the larger having multiplicity 2. SAW has only one eigenvalue and the estimate here comes from [16]. We also note here that for the (P-R-2) model although $\lambda_3 \geqslant \lambda_2$ we estimate $\nu_2 \geqslant \nu_3$. This implies that corrections to scaling are masking that $\nu_2 = \nu_3$.

	λ_1		λ_2		λ_3	
Rule	x_1	$2\nu_1$	x_2	$2\nu_2$	x_3	$2\nu_3$
SAW	1	1.184(6)	—	—	—	—
(S-C-P)	0.9995(10)	1.18(2)(2)	1.0004(6)	1.21(1)(1)	1.0007(7)	1.21(2)(3)
(P-O-3)	0.9997(4)	1.20(1)(2)	0.9999(8)	1.23(2)(1)	1.0002(5)	1.23(1)(2)
(P-2-2)	1.0002(4)	1.22(1)(1)	1.0003(5)	1.24(1)(1)	1.0002(4)	1.24(1)(2)
(P-R-2)	1.0005(14)	1.24(1)(4)	1.0015(7)	1.33(4)(7)	1.0011(6)	1.31(3)(5)
(P-P-P) 2nd	0.9997(16)	1.22(3)(2)	1.0058(20)	1.26(12)(45)	—	—
(P-P-P) 3rd	0.9991(24)	1.22(3)(7)	1.0021(26)	1.29(2)(16)	—	—

where we have used dyadic notation, and $\mathbf{1}$ is the identity tensor. Explicitly, this gives

$$\boldsymbol{I}(\varphi_n) = \sum_{i=0}^{n} \left(\begin{bmatrix} r_i^2 & 0 & 0 \\ 0 & r_i^2 & 0 \\ 0 & 0 & r_i^2 \end{bmatrix} - \begin{bmatrix} x_i x_i & x_i y_i & x_i z_i \\ y_i x_i & y_i y_i & y_i z_i \\ z_i x_i & z_i y_i & z_i z_i \end{bmatrix} \right) \tag{3.25}$$

$$= \sum_{i=0}^{N} \begin{bmatrix} y_i^2 + z_i^2 & -x_i y_i & -x_i z_i \\ -x_i y_i & x_i^2 + z_i^2 & -y_i z_i \\ -x_i z_i & -y_i z_i & x_i^2 + y_i^2 \end{bmatrix}. \tag{3.26}$$

In our enumerations we computed the expectation of the moment of inertia tensor averaging over all walks φ_n of length n, that is,

$$\langle \boldsymbol{I} \rangle_n = \frac{1}{c_n} \sum_{\varphi_n} \boldsymbol{I}(\varphi_n) \tag{3.27}$$

where the sum is over all walks, φ_n, of length n. The value of the moment of inertia depends on the origin of the coordinate system. Now, the trace of the moment of inertia tensor yields

$$\mathrm{Tr}(\langle \boldsymbol{I} \rangle_n) = \frac{1}{c_n} \sum \left(\frac{2}{n+1} \sum_{i=0}^{n} (x_i^2 + y_i^2 + z_i^2) \right) \tag{3.28}$$

which is equal to twice the mean square distance of a monomer to the endpoint if $\boldsymbol{I}$ is computed about one endpoint of the walks, or $2\langle R_g^2 \rangle$ if $\boldsymbol{I}$ is computed about the centre of mass. So, to expand on our radius of gyration enumerations, we enumerated the centre of mass $\frac{1}{n+1} \sum_{j=0}^{n} \vec{r}_j$ for each walk and then the components of the moment of inertia matrix about the centre of mass. The enumerations of the mean moment of inertia tensor computed about the centre of mass for our five models are given in appendix C.2.

In a similar manner to the analysis of the $\langle R_g^2 \rangle_n$ data, we used second-order inhomogeneous differential approximants to analyse the scaling of the eigenvalues of the mean moment of inertia tensor computed about the centre of mass, which we denote as $\lambda_1(n)$, $\lambda_2(n)$ and $\lambda_3(n)$ in ascending order of size. Note that since the trace of a matrix is the sum of its eigenvalues the scaling of the mean square monomer-to-end distance and the radius of gyration are dominated by the scaling of the largest eigenvalue. The results of this analysis are given in table 5.

These results for each of the five models indicate that the smallest eigenvalue, $\lambda_1(n)$, apparently scales with an exponent that is smaller than the exponent associated with the two larger eigenvalues. These two larger eigenvalues seem to scale with approximately the same

exponent, that is $\nu_2 = \nu_3$. The value obtained for this exponent is the same as the one obtained from the analysis of the radius of gyration. This anisotropic scaling implies that the typical walk looks like a flattened ball, and that the ball becomes flatter as the walk length increases. It is interesting to note that the degree of anisotropy in the exponents seems to be of the order of 5%, in contrast to 50% found in the two-dimensional ASSAW (and DW) models. If it were true that this anisotropy were real it would indeed be curiously subtle, and unusual, for three-dimensional critical phenomena, as far as we are aware. Intriguingly, on closer examination of the results we find that the smallest eigenvalue is also typically the best converged, and it is (with the exception of the (P-R-2) model), well converged to a SAW-like value close to 1.20 with errors that encompass the best series estimate of the unrestricted SAW model of 1.184(6). So the best converged (the biased shift in the exponent is about the same size as the statistical spread of approximants and is about 0.01) differential approximant analysis is for the smallest eigenvalue: one might expect naively that the smallest eigenvalue is affected most by corrections-to-scaling and so behaves the worst under scaling analysis. Moreover, the analyses of the largest eigenvalues have such large systematic errors that the estimate-ranges often encompass (sometimes just so) the SAW value of 1.184(6). It is then advantageous to attempt to analyse these eigenvalue scalings again with other techniques.

Because of these unusual results we then analysed the series data again, making allowances for the existence of analytic and non-analytic corrections-to-scaling by fitting to an assumed scaling form in much the same manner as [29], and as we did for the further scaling of c_n in section 3.3. In particular, we examined the cases of analytic corrections (to order $\frac{1}{n^2}$) and non-analytic corrections of the form $\frac{1}{\sqrt{n}}$ as reasonable guesses, assuming some compatibility with previous SAW work: that is, we considered

$$\lambda(n) \sim An^{2\nu}\left(1 + \frac{c_1}{n} + \frac{c_2}{n^2} + \mathrm{O}\left(\frac{1}{n^3}\right)\right) \qquad \text{as} \quad n \to \infty \tag{3.29}$$

and

$$\lambda(n) \sim An^{2\nu}\left(1 + \frac{c_2}{\sqrt{n}} + \frac{c_1}{n} + \mathrm{O}\left(\frac{1}{n^{3/2}}\right)\right) \qquad \text{as} \quad n \to \infty. \tag{3.30}$$

We did not fit directly to the above scaling form (since we did not have conjectured values of 2ν); rather we fitted to the term-by-term logarithm of the series

$$\log(\lambda(n)) = a_1 + 2\nu \log(n) + \frac{a_2}{n} + \frac{a_3}{n^2} + \mathrm{O}\left(\frac{1}{n^3}\right) \tag{3.31}$$

and

$$\log(\lambda(n)) = a_1 + 2\nu \log(n) + \frac{a_3}{\sqrt{n}} + \frac{a_2}{n} + \mathrm{O}\left(\frac{1}{n^{3/2}}\right). \tag{3.32}$$

The (linear) fits were then examined on the basis of the stability of the coefficients. For each of these two forms above the exponent 2ν was either allowed to be free, fixed at a SAW-like value of 1.19, or fixed to the apparent differential approximant calculated estimate obtained previously (1.29 for the 3D-spiral models and 1.23 for the new class).

We illustrate this analysis in more detail for (P-P-P) walks.

3.4.1. Exact fitting to corrections-to-scaling for (P-P-P) model. For the (P-P-P) model the mean inertia tensor takes the form

$$\langle \boldsymbol{I} \rangle_{(PPP)} = \begin{bmatrix} a & b & -b \\ b & a & b \\ -b & b & a \end{bmatrix} \tag{3.33}$$

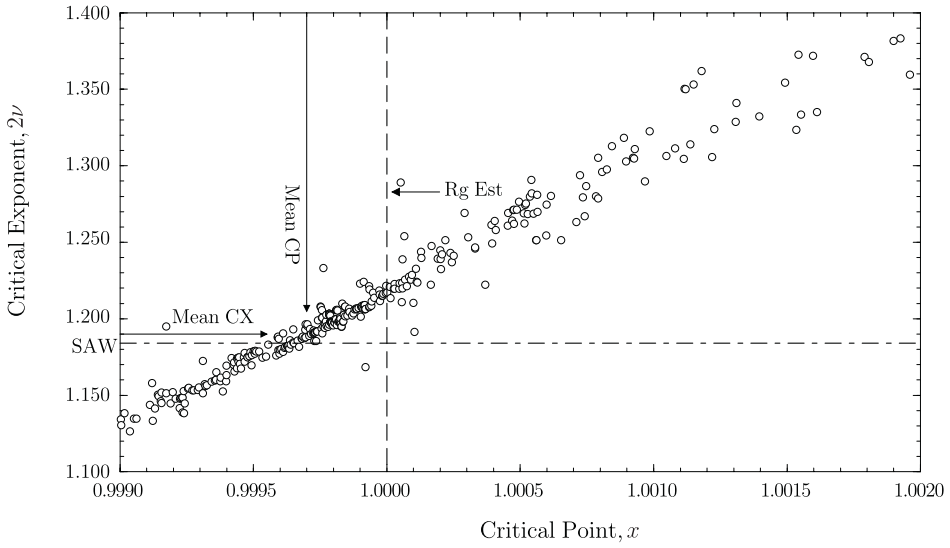

Figure 10. A plot of the λ_1 (smallest eigenvalue of the moment of inertia tensor) differential approximants for the (P-P-P), which estimate the exponent 2ν. The mean value of the critical points and exponents of these approximants is indicated. The vertical dashed line is simply the $x = 1$ (correct) critical point, while the horizontal dashed line marks the SAW value of the exponent 2ν. The estimate of the exponent from the radius of gyration analysis, Rg Est, is also marked.

and such a matrix has the following eigenvalues, λ_j, and eigenvectors, $\vec{\phi}_j$:

$$\lambda_1 = a - 2b \qquad \text{and} \qquad \{\vec{\phi}_1 = [1, -1, 1]\} \tag{3.34}$$

and

$$\lambda_2 = a + b \qquad \text{and} \qquad \{\vec{\phi}_2 = [-1, 0, 1], \vec{\phi}_3 = [1, 1, 0]\}. \tag{3.35}$$

The first interesting feature to notice is that this rule is not automatically isotropic, unlike the 2D-spiral (P) class model.

Differential approximant analysis on the two eigenvalues of the (P-P-P) model yielded (see table 5 and figure 10):

$$\lambda_1 \sim A_1 n^{2\nu_1} \qquad \text{as} \quad n \to \infty \qquad \text{with} \quad 2\nu_1 \approx 1.22(5) \tag{3.36}$$

$$\lambda_2 = \lambda_3 \sim A_3 n^{2\nu_3} \qquad \text{as} \quad n \to \infty \qquad \text{with} \quad 2\nu_3 \approx 1.29(18) \tag{3.37}$$

where the errors quoted here are simply the sum of the statistical and systematic errors. The central estimates of the exponents imply that (P-P-P) walks scale anisotropically, and that the typical walk is shaped like a flattened ball, shorter in the [1, −1, 1] direction, with a preferred plane normal to this. Since one eigenvalue apparently scales with a smaller exponent the ball becomes flatter as the walks become longer. Since the radius of gyration is the sum of the eigenvalues (up to a constant), the scaling of $\langle R_g^2 \rangle_n$ is dominated by the scaling of the largest and less well-converged eigenvalues; this translates into the relatively poor convergence of the $\langle R_g^2 \rangle_n$ series data for this model. On the other hand, both estimates' ranges include the SAW value of 1.19. So we might conclude that it is simply the case that the larger eigenvalues are afflicted with large corrections-to-scaling.

As mentioned above, it would be an unusual result if the walks scale as three-dimensional SAWs in one direction, and differently in the other two. To explore this result further we tried to fit the eigenvalues directly to the scaling forms given by equations (3.29) and (3.30), in much

the same way as [29], to examine the possible corrections-to-scaling. The results of these fits are given in appendix D.2. In summary, the smallest eigenvalue is fitted best with standard $\frac{1}{n}$ corrections with a dominant exponent close to the unrestricted SAW value, in agreement with the differential approximant analysis. However, the larger eigenvalue can also be fitted with an exponent of $2\nu = 1.19$, which is close to the unrestricted SAW value, if $\frac{1}{\sqrt{n}}$ corrections (as in (3.30)) are added, and moreover, this is arguably the best fit of six attempted for the larger eigenvalue. Hence one can argue sensibly from these fits that a SAW-like exponent is not only consistent with, but rather the best value (of those tried) for all the eigenvalues of the (P-P-P) model. See appendix D.2 for further details.

Similar results have been obtained for the other four models: (P-O-3), (P-R-2), (S-C-P) and (P-2-2). In particular, we see that the fitted values for ν drop with increasing n with either $\frac{1}{n}$ or $\frac{1}{\sqrt{n}}$ corrections, suggesting that the differential approximant estimates (particularly for the larger eigenvalues) are too high.

We therefore can conclude from the above analyses that strong corrections-to-scaling occur in the scaling of largest eigenvalues of the moment of inertia (and hence in the radius of gyration) of the models in the apparent new universality class and also those in the 3D-spiral class. Furthermore, by including such corrections into the analysis the enumeration data is consistent with there being only one scaling exponent, namely that of the unrestricted SAW.

4. Discussion

We now review the various analyses and conflicting conclusions made from those above analyses to come to some global conclusions. In the TSRW models we have examined, the radius of gyration data confirms an earlier suggestion [14] of a three-dimensional spiral universality class. Our data also supports the new suggestion that there is at least one other novel class. Poor convergence of the series analyses, based upon differential approximants, makes this conclusion contentious however. On the other hand, examination of the number of walks, c_n, again using differential approximants, seems to indicate that all the models considered have approximately the same value (within error) of their entropic exponent γ and, further, that the scaling of c_n does not contain $e^{\sqrt{n}}$ or $e^{n^{2/3}}$ factors that may invalidate the differential approximant analyses. Moreover, the symmetries of the walk rules offer little insight into the differences in their $\langle R_g^2 \rangle_n$ scaling, in distinction to two dimensions. The turning number of the rule, which we have defined here, does seem to be a better candidate as a microscopic criterion to differentiate the scaling behaviours of the TSRW models, though this too is problematic. Our examination of the scaling of the eigenvalues of the inertia tensor for five of the models indicates that the smallest eigenvalue is the best behaved numerically and, further, that it scales with an exponent quite close to that of the SAW universality class. While the analyses of the larger eigenvalues seem to be hampered by relatively larger corrections-to-scaling, they reflect the analysis of the radius of gyration which gives an exponent central-estimate larger than the SAW value. However, further analysis of the larger eigenvalues are *also consistent* with lower SAW-like values of the exponents.

The above facts leave us with a couple of alternate and reasonable conclusions. Of course, there are other possibilities given the moderate size of some of the errors on our analyses but the following are the most likely, consistent, and simplest conclusions. Either

(1) all the TSRW models in three dimensions we examined (and probably all symmetric-mixing rules) are members of the unrestricted SAW universality class with different corrections-to-scaling (categorized maybe by the turning number) or
(2) the walk rules split into at least three universality classes with different values of the

exponent ν. The non-SAW-like classes have anisotropic exponents which are only slightly anisotropic (of the order of 5%). Moreover, all classes have one exponent (the smallest) that takes on a value very close to the 3D-SAW one.

Also, we conclude that the exponent γ for any of the TSRW models examined (and presumably all symmetric-mixing models) probably takes on the SAW value (around 1.16) or a value very close to it.

Now, given our further analysis of the moment of inertia eigenvalues the weight of evidence favours the first conclusion, we believe. In any event it would be advantageous indeed to have confirmation of some of these results using Monte Carlo simulations.

Acknowledgments

ALO is grateful to the Australian Research Council for financial support and AR thanks the University of Melbourne for an Australian Postgraduate Award. We thank A J Guttmann and W Orrick for carefully reading the manuscript and making several useful suggestions.

Appendix A. Square lattice balanced and reverse-balanced walk rules

Starting with the unrestricted SAW rule in two dimensions and deleting possible moves, whilst imposing the balance and reverse-balance condition, one arrives at all the interesting rules first: being SAW (rule 1) and other SAW-like rules (rules 2, 3 and possibly 4), *spiral* (rule 7), *three-choice* (rule 5), *two-choice* (rule 6(a)) and *reverse-two-choice* (rule 6(b)). That is, these rules have the most continuing steps, as one might expect—all these rules have, at most four, missing continuing steps. We provide in figure A1 a complete list of all the distinct (up to rotations, reflections and reversals) symmetric-balanced rules starting with the rules with the most continuing steps. In constructing this list we have found a new walk rule, which we informally call the *anti-spiral* (rule 4). From our enumerations we have placed this model tentatively in class S, although another possibility is that it belongs to a novel universality class. On the other hand, others [30] argue that this rule should be in class D. We are currently analysing longer enumerations of this rule† [31,32]. A summary of the universality classes of the contents of the figure A1 is given in table A1.

Table A1. The 80 two-dimensional balanced and reverse-balanced walk rules form a total of seven (possibly eight) universality classes. The anti-spiral (rule 4) may be either in a novel universality class (N) or be a slowly converged element of the unrestricted SAW (S) class.

Universality class	$\nu_{\parallel}$	$\nu_{\perp}$	Number of rules	Distinct rules
SAW (S)	$\frac{3}{4}$	$\frac{3}{4}$	4	3
Anti-spiral (N)	$\approx$0.8	$\approx$0.6	4	1
ASSAW (A)	0.955(2)	0.4775(10)	12	2
Spiral (P)	$\frac{1}{2}$(log)	$\frac{1}{2}$(log)	2	1
DW (D)	1	$\frac{1}{2}$	6	2
Pseudo-1D (U)	1	1	19	5
1D (O)	1	0	24	6
Trivial (T)	0	0	9	4

† *Note added in proof.* Series analysis of the longest series generated (50 terms) seems to indicate that anti-spirals is a separate universality class. However, our preliminary Monte Carlo results up to length 8192 imply that the rule may indeed be directed, or close to it, which in turn implies that a slight modification of the 'mixing' condition may be necessary in two dimensions.

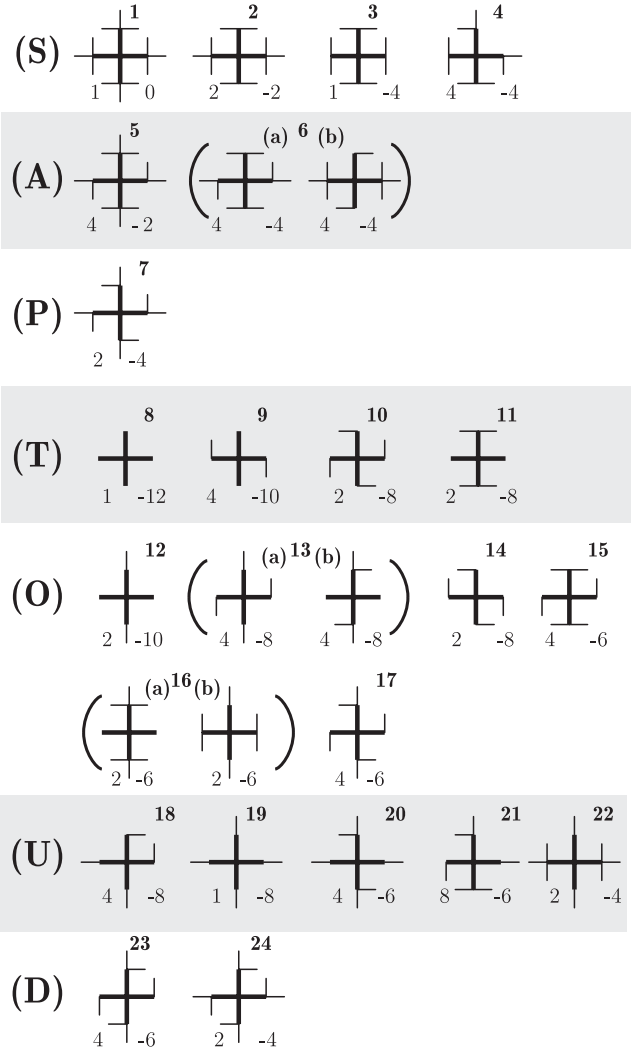

Figure A1. Diagrams of all 24 distinct (up to rotations, reflections and reversals) balanced TSRW rules on the square lattice. The rules are classified according to their apparent universality class. Each pair of rules 6(a) and 6(b), rules 13(a) and 13(b), and rules 16(a) and 16(b) are simply reversals (traversing the rule backwards) of each other respectively. We have assigned each distinct rule a number label (in bold) above each pictogram, and indicated below each rule both the degeneracy of the rule on the left and on the right the number of continuing steps that have to be removed from the unrestricted SAW rule to give that rule (e.g. -4 means four steps need to be removed).

Appendix B. Number of symmetric-balanced rules

Appendix B.1. Calculating the total number of balanced rules

For a rule to be balanced we require that there are the same number of continuing steps in the positive component as in the negative component of each axial direction. On the d-dimensional hypercubic lattice there are a total of $2d - 1$ different possible continuing steps in each of the positive and negative components of each axial direction.

To obtain a balanced rule with k continuing steps in some positive axial direction we hence require that there be k continuing steps in the negative axial direction. There are $\binom{2d-1}{k}$ ways of choosing the former set of k steps, and the same number of ways of choosing the latter set of k steps. Hence

$$\text{the number of choices of } k \text{ pairs of steps} = \binom{2d-1}{k}^2. \tag{B.1}$$

We can sum this over k to get the number of rules that are balanced with respect to that axis:

$$\sum_{k=0}^{2d-1} \binom{2d-1}{k}^2 = \binom{4d-2}{2d-1}. \tag{B.2}$$

Since there are d directions on the hypercubic lattice we obtain the following result:

$$\text{the number of balanced rules on the hypercubic lattice} = \binom{4d-2}{2d-1}^d. \tag{B.3}$$

However, there are rules that are balanced that are not reverse-balanced, and hence we wish to calculate the cardinality of the symmetric-balanced rule space.

Appendix B.2. Calculating the number of symmetric-balanced rules sorted according to the number of TSCs

In this section we do two things simultaneously: we count the number of symmetric-balanced rules and further we sort them according to the number of TSCs the rule contains. To do this we will introduce suitable generating functions. To accomplish the first task we make use of MacMahon's $\underset{=}{\overset{\lambda}{\Omega}}$ operator [33], which is a 'constant term' operator (see below).

We show here in detail the analysis for square lattice TSRW and then just state the result for higher-dimensional hyper-cubic lattices. We first write the $\boldsymbol{M}$ matrix for two dimensions (in the manner described in section 2) as

$$\boldsymbol{M} = \begin{bmatrix} \boldsymbol{rr} & 0 & \boldsymbol{rf} & \boldsymbol{rb} \\ 0 & \boldsymbol{ll} & \boldsymbol{lf} & \boldsymbol{lb} \\ \boldsymbol{fr} & \boldsymbol{fl} & \boldsymbol{ff} & 0 \\ \boldsymbol{br} & \boldsymbol{bl} & 0 & \boldsymbol{bb} \end{bmatrix} \tag{B.4}$$

with each variable entry taking the value of 0 or 1. That is, the TSRW rules are in bijection with matrices with binary entries constrained by the condition that the elements in the positions (1, 2), (2, 1), (3, 4) and (4, 3) are fixed to be 0. Let us call the set of all such matrices $\mathcal{M}$. The symmetric-balance conditions for the square lattice are given by

$$\sum_i M_{i,2j-1} = \sum_i M_{i,2j} \qquad j = 1, 2 \tag{B.5}$$

and

$$\sum_i M_{2j-1,i} = \sum_i M_{2j,i} \qquad j = 1, 2. \tag{B.6}$$

That is, we require the sum of the first two rows (columns) to be equal and the sum of the second two rows (columns) to be equal.

To be able to sort rules according to the number of TSCs we introduce a generating function whose variable t counts the number of TSCs. As an example, we can easily write down the TSC generating function $g_{\text{all}}(t)$ for all rules. Let us assign a variable, t, to each TSC in the rule

(which is equivalent to assigning a variable to each non-zero element of $\boldsymbol{M}$). The generating function is obtained by summing over all the possible allowed matrices $\boldsymbol{M}$, that is $\boldsymbol{M} \in \mathcal{M}$:

$$g_{\text{all}}(t) = \sum_{M \in \mathcal{M}} \prod_{(i,j)} t^{M_{i,j}} \tag{B.7}$$

$$= \prod_{(\text{allowed } i,j)} \sum_{M_{i,j}=0,1} t^{M_{i,j}} = (1+t)^{(\#\text{allowed } i,j)} \tag{B.8}$$

$$= (1+t)^{12} = \sum_{k=1}^{12} \binom{12}{k} t^k. \tag{B.9}$$

We can impose the symmetric-balance conditions by associating an additional weight with each element of $\boldsymbol{M}$ and then taking the constant term of the resultant polynomials with respect to these variables. To illustrate the method in detail, we first consider the number of balanced rules sorted according to the number of TSCs. This generalizes the result of the previous section. The TSC generating function $g_{\text{bal}}(t)$ we require is then

$$g_{\text{bal}}(t) = \sum_{M \in \mathcal{M} | (\sum_i M_{i,1} = \sum_i M_{i,2} \text{ and } \sum_i M_{i,3} = \sum_i M_{i,4})} \prod_{(i,j)} t^{M_{i,j}}. \tag{B.10}$$

We now show that this generating function $g_{\text{bal}}(t)$ can be written as the constant term of a generalized generating function $P(\mu_x, \mu_y; t)$ with respect to the new variables μ_x and μ_y. Taking the constant term of such a series is described by the action of the operators $\underset{=}{\overset{\mu_x}{\Omega}}$ and $\underset{=}{\overset{\mu_y}{\Omega}}$ defined by MacMahon [33]. The operator $\underset{=}{\overset{\lambda}{\Omega}}$ acts on a series $f(\lambda)$ so as to remove any term in which λ appears: i.e. finds the constant term (with respect to λ) of the expression upon which it acts. For example,

$$\underset{=}{\overset{\lambda}{\Omega}} \left\{ (1+x\lambda)^2 \left(1 + \frac{x}{\lambda}\right)^2 \right\} = 1 + 4x^2 + x^4. \tag{B.11}$$

In our work all the series we consider are finite: that is, they are polynomials.

We begin by rewriting the balance constraint on the sum over the rules as a Kronecker δ factor acting on an unconstrained sum. Hence we have

$$g_{\text{bal}}(t) = \sum_{M \in \mathcal{M}} \left[\prod_{i,j} t^{M_{i,j}} \delta\Big(\sum_j M_{1,j} - \sum_j M_{2,j} \Big) \delta\Big(\sum_j M_{3,j} - \sum_j M_{4,j} \Big) \right]. \tag{B.12}$$

The Kronecker δ picks out of the unconstrained (finite) sum the terms satisfying the conditions. Another way to evaluate a finite sum of the form $\sum_j a_j \delta(f(j))$ is to introduce a variable that 'counts' deviations from this constraint and takes the constant term of the resulting function. That is,

$$\sum_j a_j \delta(f(j)) = \text{constant term of } \lambda \text{ in } \sum_j a_j \lambda^{f(j)}. \tag{B.13}$$

Introducing variables μ_x and μ_y to take account of the two constraints we obtain

$$g_{\text{bal}}(t) = \underset{= =}{\overset{\mu_x \mu_y}{\Omega\Omega}} \left\{ \sum_{M \in \mathcal{M}} \left(\prod_{i,j} t^{M_{i,j}} \mu_x^{\sum_j M_{1,j} - \sum_j M_{2,j}} \mu_y^{\sum_j M_{3,j} - \sum_j M_{4,j}} \right) \right\} \tag{B.14}$$

$$= \underset{= =}{\overset{\mu_x \mu_y}{\Omega\Omega}} \{ P(\mu_x, \mu_y; t) \} \tag{B.15}$$

which also provides the definition of the function $P(\mu_x, \mu_y; t)$. Note that $P(\mu_x, \mu_y; t)$ can be constructed by forming a generating function from the set $\mathcal{M}$ by weighting the (non-zero)

elements in column 1 by μ_x and those in column 2 by $1/\mu_x$ and weighting the (non-zero) elements in column 3 by μ_y and those in column 4 by $1/\mu_y$, as well as weighting any (non-zero) element by t. Now we can easily evaluate $P(\mu_x, \mu_y; t)$ as a product in the same way we previously found $g_{\text{all}}(t)$. Hence, examining the operand $P(\mu_x, \mu_y; t)$ in more detail gives

$$P(\mu_x, \mu_y; t) = \sum_{M \in \mathcal{M}} \left(\prod_j (\mu_x t)^{M_{1,j}} \left(\frac{t}{\mu_x}\right)^{M_{2,j}} (\mu_y t)^{M_{3,j}} \left(\frac{t}{\mu_y}\right)^{M_{4,j}} \right) \tag{B.16}$$

$$= (1 + \mu_x t)^3 \left(1 + \frac{t}{\mu_x}\right)^3 (1 + \mu_y t)^3 \left(1 + \frac{t}{\mu_y}\right)^3. \tag{B.17}$$

In this case one can explicitly evaluate the constant term as

$$g_{\text{bal}}(t) = \underset{=}{\overset{\mu_x}{\Omega}} \left\{ \left(\sum_{k=0}^{3} \binom{3}{k} \mu_x t^k \right) \left(\sum_{k=0}^{3} \binom{3}{k} \frac{t}{\mu_x}^k \right) \right\} \times \underset{=}{\overset{\mu_y}{\Omega}} \left\{ \left(\sum_{k=0}^{3} \binom{3}{k} \mu_y t^k \right) \left(\sum_{k=0}^{3} \binom{3}{k} \frac{t}{\mu_y}^k \right) \right\} \tag{B.18}$$

$$= \left(\sum_{k=0}^{3} t^{2k} \binom{3}{k}^2 \right)^2. \tag{B.19}$$

The coefficient of t^n is the number of balanced configurations of $\boldsymbol{M}$ with n TSCs. Note that putting $t = 1$ recovers the result (B.3) in the case $d = 2$.

We now consider the generating function of rules that are symmetric-balanced in two dimensions. We define a generating function that counts such rules according to the number of TSCs as

$$g_{2,\text{sym-bal}}(t) = \sum_{M \in \mathcal{M}}^{*} \prod_{i,j} t^{M_{i,j}} \tag{B.20}$$

where the $*$ on the sum means that the sum is constrained by both conditions (B.5) and (B.6). Again this can be written as a multiple constant term expression,

$$g_{2,\text{sym-bal}}(t) = \underset{= = = =}{\overset{\mu_x \mu_y \lambda_x \lambda_y}{\Omega \Omega \Omega \Omega}} \{ P_{2,\text{sym-bal}}(\mu_x, \mu_y, \lambda_x, \lambda_y, t) \} \tag{B.21}$$

where

$$\begin{aligned} P_{2,\text{sym-bal}}(\mu_x, \mu_y, \lambda_x, \lambda_y; t) &= (1 + t\mu_x\lambda_x)(1 + t\mu_y\lambda_x) \left(1 + \frac{t\lambda_x}{\mu_y}\right) \\ &\times \left(1 + \frac{t}{\mu_x\lambda_x}\right) \left(1 + \frac{t\mu_y}{\lambda_x}\right) \left(1 + \frac{t}{\mu_y\lambda_x}\right) \\ &\times (1 + t\mu_x\lambda_y) \left(1 + \frac{t\lambda_y}{\mu_x}\right) (1 + t\mu_y\lambda_y) \\ &\times \left(1 + \frac{t\mu_x}{\lambda_y}\right) \left(1 + \frac{t}{\mu_x\lambda_y}\right) \left(1 + \frac{t}{\mu_y\lambda_y}\right). \end{aligned} \tag{B.22}$$

Using Maple$^{\text{TM}}$† to expand the polynomial and take the constant term, we find that

$$g_{2,\text{sym-bal}}(t) = 1 + 6t^2 + 19t^4 + 28t^6 + 19t^8 + 6t^{10} + t^{12}. \tag{B.23}$$

As constructed, the coefficient of t^n represents the number of symmetric-balanced TSRW rules made up of n TSCs. This can be explicitly seen, after some counting, from the catalogue of

† Maple$^{\text{TM}}$ is a registered trademark of Waterloo Maple Software.

appendix A. By a similar process as that outlined above we obtain the following results for three dimensions:

$$g_{3,\text{sym-bal}}(t) = \underset{=}{\Omega}^{\mu_x,\mu_y,\mu_z,\lambda_x,\lambda_y,\lambda_z} \{P_{3,\text{sym-bal}}(\mu_x, \mu_y, \mu_z, \lambda_x, \lambda_y, \lambda_z, t)\} \tag{B.24}$$

$$\begin{aligned} &= t^{30} + 15t^{28} + 177t^{26} + 1519t^{24} + 8457t^{22} + 30\,183t^{20} \\ &\quad +69\,829t^{18} + 105\,867t^{16} + 105\,867t^{14} + 69\,829t^{12} \\ &\quad +30\,183t^{10} + 8457t^8 + 1519t^6 + 177t^4 + 15t^2 + 1 \end{aligned} \tag{B.25}$$

and four dimensions:

$$g_{4,\text{sym-bal}}(t) = \underset{=}{\Omega}^{\mu_i,\lambda_i;\{i=1\ldots4\}} \{P_{4,\text{sym-bal}}(\mu_i, \lambda_i, t)\} \tag{B.26}$$

$$\begin{aligned} &= t^{56} + 28t^{54} + 738t^{52} + 16\,268t^{50} \\ &\quad +274\,907t^{48} + \cdots + 94\,001\,836\,824t^{28} \\ &\quad + \cdots + 274\,907t^8 + 16\,268t^6 + 738t^4 + 28t^2 + 1. \end{aligned} \tag{B.27}$$

Substituting $t = 1$ into the generating functions gives the total number of symmetric-balanced rules. Hence find that there are

- 80 TSRW rules in two dimensions,
- 432 096 TSRW rules in three dimensions and
- 478 340 593 664 TSRW rules in four dimensions.

Appendix C. Exact enumeration data

Appendix C.1. Radius of gyration and number of walk configuration tables

Table C1. The enumeration data, c_n and $\langle R_g^2 \rangle$, for the rules (Rot-π), (P-P-3) and (P-P-D).

	(Rot-π)		(P-P-3)		(P-P-D)	
n	c_n	$\langle R_g^2 \rangle_n$	c_n	$\langle R_g^2 \rangle_n$	c_n	$\langle R_g^2 \rangle_n$
1	6	0.250 000 0000	6	0.250 000	6	0.250 000 0000
2	18	0.518 518 5185	20	0.511 111	18	0.518 518 5185
3	54	0.787 037 0370	66	0.772 727	54	0.796 296 2963
4	158	1.062 278 481	206	1.060 971	154	1.112 727 273
5	466	1.330 591 321	652	1.352 079	446	1.444 319 880
6	1 338	1.616 180 104	2 012	1.667 018	1 266	1.810 233 098
7	3 886	1.894 042 717	6 264	1.984 924	3 626	2.189 878 654
8	11 082	2.189 255 850	19 254	2.321 767	10 282	2.598 303 160
9	31 842	2.479 427 800	59 442	2.662 321	29 262	3.020 260 406
10	90 542	2.782 749 105	182 148	3.018 780	82 790	3.467 095 379
11	258 466	3.083 967 846	559 568	3.378 845	234 674	3.925 950 941
12	733 190	3.395 616 965	1 710 476	3.752 893	662 518	4.406 914 942
13	2 084 726	3.706 346 879	5 237 592	4.130 143	1 872 906	4.897 985 755
14	5 902 350	4.026 035 244	15 980 914	4.519 812	5 279 098	5.408 667 159
15	16 738 270	4.345 208 279	48 822 216	4.912 359	14 895 186	5.927 984 092
16	47 319 166	4.672 362 374	148 757 054	5.316 068	41 934 586	6.464 774 052
17	133 935 010	4.999 214 463	453 683 704	5.722 368	118 150 286	7.009 094 165
18	378 189 902	5.333 289 679	1 380 795 336	6.138 830	332 311 930	7.569 169 389
19	1 068 895 606	5.667 227 224	4 205 655 986	6.557 627	935 234 466	8.135 866 302
20	3 015 366 794	6.007 756 322	12 788 431 474	6.985 764	2 628 389 278	8.716 905 437

Table C1. (Continued)

	(Rot-π)		(P-P-3)		(P-P-D)	
n	c_n	$\langle R_g^2\rangle_n$	c_n	$\langle R_g^2\rangle_n$	c_n	$\langle R_g^2\rangle_n$
21	8 512 718 274	6.348 276 986	38 910 558 974	7.416 014	7 390 474 750	9.303 800 493
22	23 995 774 102	6.694 862 106	118 229 769 376	7.854 911	20 756 622 062	9.903 846 043
23			359 424 2488 58	8.295 731		
24			1091 427 480 250	8.744 604		
25			3315 651 798 324	9.195 238		

Table C2. The enumeration data, c_n and $\langle R_g^2\rangle$, for the rules (S-C-3), (S-C-P), (3-3-C) and (S-P-3).

	S-C-3		(S-C-P)		(3-3-C)	
n	c_n	$\langle R_g^2\rangle_n$	c_n	$\langle R_g^2\rangle_n$	c_n	$\langle R_g^2\rangle_n$
1	6	0.250 000	6	0.250 000 0000	6	0.250 000
2	24	0.500 000	22	0.505 050 5050	22	0.505 051
3	90	0.766 667	78	0.769 230 7690	80	0.771 875
4	324	1.059 259	266	1.056 842 106	284	1.060 845
5	1 166	1.366 447	910	1.354 273 505	1 014	1.359 358
6	4 138	1.694 716	3 054	1.672 266 549	3 564	1.678 142
7	14 730	2.031 848	10 310	1.993 913 676	12 588	2.002 155
8	51 992	2.386 510	34 446	2.331 570 689	44 098	2.341 145
9	183 898	2.747 547	115 450	2.672 526 808	154 832	2.684 732
10	646 980	3.122 930	384 530	3.026 504 010	540 770	3.040 744
11	2 279 702	3.502 933	1 283 462	3.382 982 338	1 891 584	3.400 228
12	8 002 976	3.895 122	4 265 822	3.750 604 402	6 592 486	3.770 323
13	28 127 418	4.290 869	14 199 618	4.120 239 122	23 001 542	4.143 167
14	98 585 096	4.697 309	47 120 838	4.499 743 779	80 037 948	4.525 304
15	345 848 306	5.106 591	156 545 474	4.880 926 243	278 740 232	4.909 733
16	1 210 704 274	5.525 411	518 858 122	5.270 979 045	968 743 336	5.302 460
17	4 241 348 770	5.946 576	1 721 232 166	5.662 463 560	3 369 017 390	5.697 144
18	14 833 284 544	6.376 375	5 699 369 614	6.062 020 580	11 697 449 542	6.099 341
19	51 907 058 582	6.808 156	18 885 164 058	6.462 824 345	40 635 868 918	6.503 236
20	181 392 476 966	7.247 841	62 483 445 082	6.871 045 435	140 979 332 596	6.914 013
21	634 197 818 374	7.689 232	206 852 302 966	7.280 367 595		
22	2214 804 822 718	8.137 924	683 942 288 222	7.696 558 450		
23	7737 946 227 490	8.588 107				

	(S-P-3)			(S-P-3) (continued)	
n	c_n	$\langle R_g^2\rangle_n$	n	c_n	$\langle R_g^2\rangle_n$
1	6	0.250 000	10	1 105 052	2.894 842
2	24	0.500 000	11	4 165 768	3.232 301
3	96	0.752 604	12	15 635 564	3.580 525
4	368	1.029 130	13	58 773 288	3.930 671
5	1 422	1.311 260	14	220 229 536	4.290 298
6	5 392	1.612 548	15	826 135 272	4.651 580
7	20 562	1.917 156	16	3 091 645 402	5.021 351
8	77 590	2.237 052	17	11 579 713 514	5.392 576
9	293 760	2.559 677	18	43 290 642 466	5.771 503

Table C3. The enumeration data, c_n and $\langle R_g^2 \rangle$, for the rules (P-O-3), (P-3-3) and (P-2-2).

	(P-O-3)		(P-3-3)		(P-2-2)	
n	c_n	$\langle R_g^2 \rangle_n$	c_n	$\langle R_g^2 \rangle_n$	c_n	$\langle R_g^2 \rangle_n$
1	6	0.250 000 0000	6	0.250 000	3	0.250 000
2	16	0.527 777 7780	22	0.505 051	10	0.488 889
3	44	0.812 500 0000	78	0.769 231	32	0.734 375
4	112	1.147 142 857	266	1.056 842	98	1.002 449
5	290	1.489 080 460	914	1.351 872	302	1.275 754
6	730	1.862 230 920	3 072	1.670 095	905	1.572 804
7	1 858	2.238 125 673	10 388	1.992 612	2 731	1.872 414
8	4 644	2.641 571 230	34 696	2.333 659	8 121	2.190 149
9	11 692	3.045 703 045	116 326	2.677 870	24 254	2.510 089
10	29 128	3.471 307 038	387 094	3.037 176	71 801	2.844 642
11	72 866	3.898 065 933	1 291 232	3.399 126	213 168	3.181 094
12	181 092	4.342 164 570	4 285 502	3.773 997	629 044	3.530 483
13	451 246	4.787 541 630	14 247 504	4.151 048	1 860 191	3.881 363
14	1 119 492	5.247 478 820	47 195 288	4.539 472	5 476 975	4.243 746
15	2 782 326	5.708 806 865	156 532 896	4.929 770	16 151 357	4.607 443
16	6 893 472	6.182 730 795	517 758 628	5.330 238	47 474 808	4.981 465
17	17 101 294	6.658 119 150	1 714 230 392	5.732 355	139 716 218	5.356 659
18	42 325 616	7.144 718 770	5 663 536 142	6.143 698	410 143 001	5.741 247
19	104 857 966	7.632 773 830	18 725 774 596	6.556 509	1 205 156 331	6.126 905
20	259 302 146	8.131 019 980	61 809 095 034	6.977 778	3 534 113 551	6.521 186
21	641 714 298	8.630 686 255	204 143 781 018	7.400 373	10 371 867 145	6.916 460
22	1 585 767 184	9.139 738 495	673 309 667 636	7.830 787	30 389 668 612	7.319 704
23	3 921 055 588	9.650 150 405	2 221 867 592 366	8.262 410	89 099 312 437	7.723 878
24	9 683 676 170	10.169 308 00	7 323 479 170 494	8.701 308	260 877 974 233	8.135 467
25	23 927 486 656	10.689 740 44				
26	59 062 356 252	11.218 386 94				
27	145 850 988 968	11.748 222 25				
28	359 856 328 600	12.285 811 77				

Table C4. The enumeration data, c_n and $\langle R_g^2 \rangle$, for the rules (P-P-3), (P-R-2) and (P-P-P).

	(P-P-3)		(P-R-2)		(P-P-P)	
n	c_n	$\langle R_g^2 \rangle_n$	c_n	$\langle R_g^2 \rangle_n$	c_n	$\langle R_g^2 \rangle_n$
1	6	0.250 000	6	0.500 000 0000	6	0.250 000
2	20	0.511 111	18	0.987 654 3210	18	0.518 519
3	66	0.772 727	54	1.472 222 222	54	0.777 778
4	206	1.060 971	150	2.018 133 333	150	1.059 200
5	652	1.352 079	426	2.565 206 051	426	1.325 117
6	2 012	1.667 018	1 170	3.165 532 880	1 158	1.613 620
7	6 264	1.984 924	3 250	3.769 846 154	3 204	1.891 912
8	19 254	2.321 767	8 890	4.413 814 940	8 682	2.187 736
9	59 442	2.662 321	24 444	5.064 869 907	23 724	2.481 578
10	182 148	3.018 780	66 598	5.750 268 231	64 194	2.788 945

Table C4. (continued)

	(*P*-*P*-3)		(*P*-*R*-2)		(*P*-*P*-*P*)	
n	c_n	$\langle R_g^2 \rangle_n$	c_n	$\langle R_g^2 \rangle_n$	c_n	$\langle R_g^2 \rangle_n$
11	559 568	3.378 845	182 044	6.442 183 392	174 378	3.097 380
12	1 710 476	3.752 893	494 462	7.165 571 886	470 856	3.418 129
13	5 237 592	4.130 143	1 346 212	7.894 713 402	1 274 430	3.740 403
14	15 980 914	4.519 812	3 648 594	8.652 187 898	3 434 826	4.074 125
15	48 822 216	4.912 359	9 905 610	9.415 095 218	9 272 346	4.409 709
16	148 757 054	5.316 068	26 803 048	10.203 524 10	24 953 004	4.755 764
17	453 683 704	5.722 368	72 618 674	10.997 037 01	67 230 288	5.103 799
18	1 380 795 336	6.138 830	196 243 194	11.813 832 70	180 705 126	5.461 477
19	4 205 655 986	6.557 627	530 861 042	12.635 340 41	486 152 604	5.821 086
20	12 788 431 474	6.985 764	1 433 106 984	13.478 308 40	1 305 430 884	6.189 624
21	38 910 558 974	7.416 014	3 871 966 934	14.325 626 44	3 507 947 838	6.560 016
22	118 229 769 376	7.854 911	10 443 886 572	15.192 854 13	9 412 114 986	6.938 709
23	359 424 248 858	8.295 731	28 189 364 062	16.064 111 32	25 268 587 338	7.319 174
24	1 091 427 480 250	8.744 604	75 981 934 450	16.953 929 65	67 752 451 146	7.707 392
25	3 315 651 798 324	9.195 238	204 918 079 282	17.847 496 54	181 754 458 194	8.097 294
26			552 010 606 124	18.758 448 67	487 060 621 596	8.494 472
27					1 305 761 069 730	8.893 243
28					3 497 441 209 182	9.298 868
29					9 371 171 057 352	9.705 999

Appendix C.2. Moment of inertia eigenvalue enumeration tables

Table C5. Eigenvalues of the moment of inertia tensor computed about the centre of mass for the (*S*-*C*-*P*) and (*P*-*O*-3) rules.

	(*S*-*C*-*P*)			(*P*-*O*-3)		
n	λ_1	λ_2	λ_3	λ_1	λ_2	λ_3
1	0.166 666 6667	0.166 666 6667	0.166 666 6667	0.166 666 666 667	0.166 666 666 667	0.166 666 666 667
2	0.323 232 3232	0.323 232 3232	0.363 636 3636	0.302 276 833 646	0.364 389 833 021	0.388 888 888 889
3	0.483 974 3590	0.583 698 4453	0.470 788 7341	0.426 824 397 156	0.569 876 200 940	0.628 299 401 917
4	0.655 639 0977	0.828 126 5757	0.629 918 5371	0.566 948 065 248	0.814 084 994 660	0.913 252 654 398
5	0.832 112 3321	1.083 682 865	0.792 751 8113	0.698 817 526 155	1.070 556 537 65	1.208 786 855 77
6	1.018 670 730	1.358 246 075	0.967 616 2926	0.834 240 876 666	1.355 020 019 27	1.535 200 943 59
7	1.206 237 876	1.636 945 906	1.144 643 570	0.965 014 568 266	1.645 397 903 96	1.865 838 873 37
8	1.401 436 351	1.930 158 848	1.331 546 178	1.099 432 345 75	1.959 679 651 42	2.224 030 461 99
9	1.597 762 148	2.226 718 876	1.520 572 592	1.231 125 090 25	2.275 865 782 03	2.584 415 217 38
10	1.800 378 395	2.535 047 728	1.717 581 896	1.366 397 733 24	2.609 951 498 21	2.966 264 844 68
11	2.003 823 794	2.845 912 484	1.916 228 398	1.500 162 391 82	2.945 275 123 99	3.350 694 348 86
12	2.212 733 910	3.166 808 488	2.121 666 404	1.637 510 267 26	3.294 511 564 12	3.752 307 308 27
13	2.422 322 095	3.489 717 948	2.328 438 200	1.773 864 371 45	3.644 753 004 86	4.156 465 882 92
14	2.636 818 108	3.821 491 853	2.541 177 597	1.913 616 593 94	4.006 362 098 65	4.574 978 949 01
15	2.851 890 731	4.154 931 390	2.755 030 364	2.052 685 535 96	4.368 998 234 18	4.995 929 957 07

Table C5. (Continued)

	(*S*-*C*-*P*)			(*P*-*O*-3)		
n	λ_1	λ_2	λ_3	λ_1	λ_2	λ_3
16	3.071 423 508	4.496 325 628	2.974 208 952	2.194 877 047 34	4.741 315 122 04	5.429 269 420 78
17	3.291 456 083	4.839 133 151	3.194 337 891	2.336 591 985 58	5.114 735 889 58	5.864 910 421 51
18	3.515 583 085	5.189 171 582	3.419 286 494	2.481 171 037 22	5.496 714 705 89	6.311 551 793 34
19	3.740 151 811	5.540 434 799	3.645 062 085	2.625 406 338 02	5.879 824 996 05	6.760 316 323 78
20	3.968 508 782	5.898 336 079	3.875 246 007	2.772 280 501 71	6.270 705 848 16	7.219 053 612 38
21	4.197 260 774	6.257 314 900	4.106 159 520	2.918 908 723 88	6.662 718 345 26	7.679 745 437 12
22	4.429 540 412	6.622 436 345	4.341 140 145	3.067 979 455 86	7.061 900 675 32	8.149 596 855 36
23				3.216 874 07350	7.462 185 18484	8.621 241 553 10
24				3.368 049 06946	7.869 170 66793	9.101 396 265 25
25				3.519 095 21920	8.277 201 72517	9.583 183 929 35
26				3.672 284 51329	8.691 546 94518	10.072 942 421 8
27				3.825 380 54292	9.106 874 38372	10.564 189 568 9
28				3.980 500 21705	9.528 180 50950	11.062 942 810 1

Table C6. Eigenvalues of the moment of inertia tensor computed about the centre of mass for the (*P*-2-2) and (*P*-*R*-2) rules.

	(*P*-2-2)			(*P*-*R*-2)		
n	λ_1	λ_2	λ_3	λ_1	λ_2	λ_3
1	0.166 666 6667	0.166 666 6667	0.166 666 6667	0.166 666 6667	0.166 666 6667	0.166 666 6667
2	0.306 116 7806	0.311 111 1111	0.360 549 8861	0.294 292 8684	0.320 987 6543	0.372 373 7985
3	0.438 060 3326	0.457 031 2500	0.573 658 4178	0.411 636 1451	0.476 944 4645	0.583 641 6133
4	0.576 854 9300	0.617 142 8575	0.810 900 1732	0.533 599 7647	0.653 970 4927	0.830 563 0769
5	0.714 782 7913	0.780 150 7133	1.056 574 958	0.651 574 8546	0.833 657 2627	1.079 973 934
6	0.861 990 2703	0.958 634 1077	1.324 983 923	0.774 523 3588	1.034 225 881	1.356 783 641
7	1.008 795 944	1.138 534 983	1.597 496 983	0.895 978 6064	1.237 000 753	1.636 866 796
8	1.162 874 755	1.330 319 099	1.887 103 536	1.021 468 006	1.455 531 410	1.936 815 524
9	1.317 037 920	1.523 442 032	2.179 698 169	1.146 692 636	1.677 217 902	2.240 959 373
10	1.477 216 020	1.725 865 771	2.486 202 909	1.276 102 492	1.912 047 787	2.562 117 957
11	1.637 644 958	1.929 534 679	2.795 008 619	1.405 388 728	2.149 897 142	2.886 897 521
12	1.803 541 690	2.141 291 486	3.116 133 542	1.538 733 190	2.399 671 785	3.227 166 913
13	1.969 670 042	2.354 060 265	3.438 996 579	1.672 079 918	2.652 093 350	3.570 540 133
14	2.140 712 992	2.573 986 173	3.772 793 127	1.809 124 263	2.915 259 538	3.927 804 101
15	2.312 008 455	2.794 817 983	4.108 059 365	1.946 291 614	3.180 868 289	4.287 935 315
16	2.487 741 851	3.022 057 624	4.453 129 695	2.086 834 798	3.456 143 376	4.660 545 924
17	2.663 728 951	3.250 112 163	4.799 476 692	2.227 556 192	3.733 680 281	5.035 800 539
18	2.843 771 098	3.483 990 690	5.154 731 719	2.371 400 424	4.020 017 670	5.422 414 610
19	3.024 065 642	3.718 614 760	5.511 129 042	2.515 443 402	4.308 440 799	5.811 456 215
20	3.208 093 348	3.958 584 700	5.875 693 123	2.662 393 290	4.604 966 665	6.210 948 447
21	3.392 371 559	4.199 246 804	6.241 301 327	2.809 548 671	4.903 410 105	6.612 667 668
22	3.580 107 306	4.444 850 763	6.614 449 240	2.959 418 683	5.209 367 525	7.024 067 925
23	3.768 090 188	4.691 102 500	6.988 563 927	3.109 495 958	5.517 093 898	7.437 521 480
24	3.959 295 468	4.941 953 028	7.369 686 415	3.262 117 597	5.831 822 352	7.859 989 694
25				3.414 944 831	6.148 190 665	8.284 361 061
26				3.570 166 948	6.471 113 948	8.717 167 785

Table C7. Eigenvalues of the moment of inertia tensor computed about the centre of mass for the (P-P-P) rule. Note that the largest eigenvalue of the (P-P-P) model has degeneracy of 2.

	(P-P-P)	
n	λ_1	$\lambda_2 = \lambda_3$
1	0.166 666 6667	0.166 666 6667
2	0.345 679 0123	0.345 679 0123
3	0.509 259 2595	0.523 148 1481
4	0.674 133 3341	0.722 133 3334
5	0.818 205 5301	0.916 014 6058
6	0.962 673 1535	1.132 282 965
7	1.094 159 643	1.344 832 631
8	1.225 643 519	1.574 914 466
9	1.352 100 826	1.805 527 734
10	1.479 217 568	2.049 336 503
11	1.604 029 273	2.295 365 288
12	1.730 382 624	2.552 937 955
13	1.855 199 371	2.812 803 563
14	1.981 875 267	3.083 187 469
15	2.107 554 467	3.355 931 295
16	2.235 127 971	3.638 200 261
17	2.362 027 099	3.922 785 165
18	2.490 795 277	4.216 079 012
19	2.619 076 033	4.511 547 856
20	2.749 167 507	4.815 040 036
21	2.878 906 185	5.120 562 709
22	3.010 385 583	5.433 515 799
23	3.141 610 116	5.748 368 769
24	3.274 505 289	6.070 139 649
25	3.407 213 837	6.393 687 511
26	3.541 525 172	6.723 709 674
27	3.675 698 752	7.055 393 692
28	3.811 409 808	7.393 163 447

Appendix D. Tables of fits to scaling forms

In this section we include the tables of coefficients from the exact local fittings of various scaling forms for both the numbers of walk configurations and the eigenvalues of the moment of inertia tensor.

Appendix D.1. Exact fitting analysis of the number of walk configurations

In table D1 there are the results of three fits to the numbers of walks, c_n for the (P-P-P) model. The top third of the table gives the coefficients of a linear fit using n, $n-2$ and $n-4$ for $n = 20, \ldots, 28$ to the form (3.20), which is the canonical scaling form for SAWs. The middle of the table and the bottom give similar fits to the forms (3.21) and (3.22) respectively, using one more term, $n-6$, per fit. In each case the value of the exponent γ is allowed to vary. In table D2 the same three fitting forms are used but this time the value of the exponent γ is fixed to be the (exact enumeration) SAW estimate of 1.161 at each n (and hence one less term of the series is needed for the fit at each length). In both cases the addition of $\frac{1}{\sqrt{n}}$ or $\frac{1}{n^{2/3}}$ corrections only worsen the stability of the other coefficients (slightly). More to the point, the

coefficients of these corrections are small in all cases and though quite unstable, they appear to be decreasing in magnitude as n increases (but not monotonically). Given their apparent size, it is likely that these corrections are spurious. Whether a value of γ closer to 1.16 or 1.19 produces a better fit is a matter for debate. We have included both fits for completeness.

Table D1. Linear fit of the enumerations, c_n, for the rule (P-P-P), to various scaling forms, with and without corrections.

n	a_1	$\log \mu$	$\gamma - 1$	Corrections	a_2
20	0.832 475 6081	0.978 319 2165	0.197 260 3078		
21	0.845 548 8938	0.978 544 0966	0.191 597 2483		
22	0.837 339 9541	0.978 451 1613	0.194 755 6593		
23	0.848 323 9152	0.978 613 7500	0.190 205 3258		
24	0.840 952 9395	0.978 535 4534	0.192 986 8688		
25	0.850 388 7379	0.978 658 7025	0.189 217 0502		
26	0.843 969 5129	0.978 596 9601	0.191 573 1899		
27	0.852 066 7855	0.978 690 8435	0.188 446 1032		
28	0.846 688 3266	0.978 646 0255	0.190 347 1629		
20	0.838 693 0908	0.981 325 1606	0.251 171 6395	$\sqrt{n}$	−0.050 946 6361
21	0.847 017 6349	0.979 819 4475	0.215 746 8764	$\sqrt{n}$	−0.022 209 1673
22	0.837 767 6328	0.980 877 7278	0.243 147 0492	$\sqrt{n}$	−0.043 363 3175
23	0.847 182 7158	0.979 964 4881	0.218 495 4545	$\sqrt{n}$	−0.024 735 9243
24	0.837 659 4009	0.980 255 6927	0.230 740 6980	$\sqrt{n}$	−0.032 246 6960
25	0.847 468 4875	0.979 623 5445	0.211 356 9120	$\sqrt{n}$	−0.018 493 2533
26	0.838 195 5848	0.979 975 6433	0.224 594 4906	$\sqrt{n}$	−0.026 997 0353
27	0.848 012 0233	0.979 444 1350	0.207 239 6293	$\sqrt{n}$	−0.015 054 3115
28	0.838 737 4396	0.979 846 2623	0.221 495 6491	$\sqrt{n}$	−0.024 463 5323
20	0.816 766 9269	0.982 875 9076	0.238 115 2320	$n^{\frac{2}{3}}$	−0.026 847 7019
21	0.837 536 6772	0.980 471 0583	0.209 841 1804	$n^{\frac{2}{3}}$	−0.011 560 9483
22	0.819 351 4045	0.982 126 2157	0.231 393 5557	$n^{\frac{2}{3}}$	−0.022 430 5704
23	0.836 763 3784	0.980 657 0383	0.211 601 9897	$n^{\frac{2}{3}}$	−0.012 676 7502
24	0.824 191 8436	0.981 137 3146	0.221 534 8590	$n^{\frac{2}{3}}$	−0.016 394 8459
25	0.839 815 7465	0.980 117 4498	0.205 951 9375	$n^{\frac{2}{3}}$	−0.009 329 1643
26	0.827 104 4829	0.980 684 7143	0.216 570 7673	$n^{\frac{2}{3}}$	−0.013 543 2894
27	0.841 907 8052	0.979 828 8918	0.202 641 2139	$n^{\frac{2}{3}}$	−0.007 483 6755
28	0.828 970 2197	0.980 453 8038	0.213 805 7326	$n^{\frac{2}{3}}$	−0.012 045 3271

Table D2. Linear fit of the enumerations, c_n, for the rule (P-P-P), to various scaling forms, with and without corrections, and with γ fixed at the SAW value.

n	a_1	$\log \mu$	$\gamma - 1$	Corrections	a_2
20	0.902 897 8209	0.980 229 4140	0.161		
21	0.906 548 9941	0.980 075 2350	0.161		
22	0.906 290 2192	0.980 059 7940	0.161		
23	0.909 343 2958	0.979 942 1730	0.161		
24	0.909 210 3892	0.979 927 0590	0.161		
25	0.911 806 0176	0.979 835 0981	0.161		
26	0.911 766 8293	0.979 820 5410	0.161		
27	0.914 008 5907	0.979 746 9950	0.161		

Table D2. (Continued)

n	a_1	$\log \mu$	$\gamma - 1$	Corrections	a_2
28	0.914 031 1693	0.979 733 4510	0.161		
20	0.828 292 9603	0.976 297 3926	0.161	$\sqrt{n}$	0.034 266 6881
21	0.843 696 0392	0.976 928 6659	0.161	$\sqrt{n}$	0.028 135 0308
22	0.837 043 4575	0.976 758 5843	0.161	$\sqrt{n}$	0.030 247 5055
23	0.849 493 2420	0.977 218 8950	0.161	$\sqrt{n}$	0.025 539 9818
24	0.843 739 1859	0.977 077 7906	0.161	$\sqrt{n}$	0.027 322 7611
25	0.854 119 9161	0.977 429 4158	0.161	$\sqrt{n}$	0.023 565 6305
26	0.849 322 5760	0.977 320 7765	0.161	$\sqrt{n}$	0.024 992 6735
27	0.857 989 9424	0.977 590 8142	0.161	$\sqrt{n}$	0.021 984 6353
28	0.854 178 9041	0.977 515 1871	0.161	$\sqrt{n}$	0.023 048 9648
20	0.846 417 0165	0.974 274 8997	0.161	$n^{\frac{2}{3}}$	0.023 828 6629
21	0.858 986 3846	0.975 312 3551	0.161	$n^{\frac{2}{3}}$	0.019 389 0739
22	0.853 915 7434	0.975 065 4537	0.161	$n^{\frac{2}{3}}$	0.020 665 0354
23	0.864 099 4381	0.975 824 3720	0.161	$n^{\frac{2}{3}}$	0.017 304 7187
24	0.859 729 9761	0.975 619 8890	0.161	$n^{\frac{2}{3}}$	0.018 370 9537
25	0.868 223 9511	0.976 199 7433	0.161	$n^{\frac{2}{3}}$	0.015 727 2307
26	0.864 604 4552	0.976 044 2026	0.161	$n^{\frac{2}{3}}$	0.016 561 1703
27	0.871 711 1764	0.976 490 6343	0.161	$n^{\frac{2}{3}}$	0.014 468 7926
28	0.868 851 0450	0.976 384 2349	0.161	$n^{\frac{2}{3}}$	0.015 069 9597

Appendix D.2. Exact fitting analysis of the moment of inertia eigenvalues

In tables D3 and D4 are the fits to the smallest eigenvalue, $\lambda_1(n)$, of the moment of inertia matrix for the (P-P-P) model using the forms (3.31) and (3.32) respectively. The form (3.31) includes $\frac{1}{n}$ type corrections while the form (3.32) includes $\frac{1}{\sqrt{n}}$ type corrections. The number of terms of the series used varied according to the number of free coefficients: e.g., if there were three free coefficients then the three terms n, $n-2$ and $n-4$ were utilized. In both cases the top of the table gives coefficients for fits where the value of $2\nu_1$ is free, while the middle and bottom sections give coefficients that have $2\nu_1$ fixed. We tried two fixed values: the SAW estimate of 1.19 and the best $\langle R_g^2 \rangle_n$ differential approximant estimate for the (P-P-P) model of 1.29. Coefficients from fits for $n = 20$ to $n = 28$ are included. The standard correction fit in table D3, with $2\nu_1$ free, gives values of $2\nu_1$ close to the SAW value, if slightly increasing. The coefficient, a_2, of the $\frac{1}{n}$ term is less stable if the value of $2\nu_1$ is fixed at 1.29 than if it is fixed at 1.19 or allowed to be free. Note that the value of a_2 is only affected a little by the change from free to fixed at 1.19. All the fits in table D4 that use the $\frac{1}{\sqrt{n}}$-type corrections are less stable than those in table D3 that use the $\frac{1}{n}$ corrections. In particular, the coefficient a_2 is far less stable. This implies that the best fit concurs with the differential approximant analysis with a value of $2\nu_1$ around 1.19, and uses the relatively benign $\frac{1}{n}$ corrections. This second point concurs with the observation that the differential approximants of the smallest eigenvalue, $\lambda_1(n)$, were relatively well behaved.

In tables D5 and D6 are the fits to the largest eigenvalue, $\lambda_3(n)$, of the moment of inertia matrix for the (P-P-P) model using the forms (3.31) and (3.32) respectively. Once again, the top of the tables give coefficients for the fits where the value of $2\nu_3$ is free while the middle and bottom coefficients have $2\nu_3$ fixed, as for $\lambda_1(n)$. The fit with $\frac{1}{n}$ corrections and $2\nu_3$ free

Table D3. The coefficients of three fits to the smallest eigenvalue, $\lambda_1(n)$, of the moment of inertia for the $(P\text{-}P\text{-}P)$ model. The top fit allows the value of ν to be free while the bottom two fits fix this exponent. These fits use $\frac{1}{n}$ corrections: see equation (3.31).

n	a_1	$2\nu_1$	a_2	a_3
20	−2.724 815 224	1.163 388 477	5.666 275 943	−12.960 334 92
21	−2.749 265 119	1.169 014 693	5.858 321 147	−13.840 165 15
22	−2.774 577 794	1.174 725 610	6.073 152 086	−14.778 035 77
23	−2.793 298 510	1.178 924 259	6.233 843 907	−15.612 340 80
24	−2.814 179 170	1.183 535 931	6.424 678 029	−16.525 350 92
25	−2.826 827 330	1.186 303 333	6.543 063 127	−17.227 132 64
26	−2.836 927 800	1.188 491 651	6.642 284 471	−17.716 431 62
27	−2.846 262 248	1.190 496 482	6.735 594 254	−18.329 353 42
28	−2.852 661 690	1.191 855 454	6.803 456 388	−18.679 478 25
20	−2.841 622 425	1.19	6.621 334 854	−17.227 033 37
21	−2.842 513 608	1.19	6.653 550 396	−17.592 989 74
22	−2.843 234 486	1.19	6.682 593 176	−17.807 375 37
23	−2.843 624 178	1.19	6.697 973 178	−18.036 106 99
24	−2.843 851 650	1.19	6.708 514 087	−18.078 927 76
25	−2.843 960 818	1.19	6.712 785 354	−18.198 704 28
26	−2.843 982 848	1.19	6.714 549 189	−18.148 200 23
27	−2.843 920 033	1.19	6.710 827 665	−18.175 252 76
28	−2.843 834 255	1.19	6.707 119 559	−18.055 478 48
20	−3.280 556 421	1.29	10.210 203 81	−33.260 104 93
21	−3.286 864 991	1.29	10.443 009 45	−35.476 110 16
22	−3.292 724 237	1.29	10.672 580 83	−37.640 518 79
23	−3.298 000 706	1.29	10.888 438 06	−39.919 260 59
24	−3.302 886 931	1.29	11.099 414 00	−42.112 104 40
25	−3.307 447 054	1.29	11.304 077 40	−44.481 846 98
26	−3.311 730 277	1.29	11.506 207 91	−46.781 390 96
27	−3.315 754 269	1.29	11.702 823 70	−49.258 495 39
28	−3.319 594 507	1.29	11.899 419 41	−51.688 670 47

Table D4. The coefficients of three fits to the smallest eigenvalue, $\lambda_1(n)$, of the moment of inertia for the $(P\text{-}P\text{-}P)$ model. The top fit allows the value of ν to be free while the bottom two fits fix this exponent. These fits use $\frac{1}{\sqrt{n}}$ corrections: see equation (3.32).

n	a_1	$2\nu_1$	a_2	a_3
20	−4.463 970 915	1.438 199 488	−3.606 651 092	6.024 597 655
21	−4.417 089 672	1.430 174 649	−3.480 093 584	5.893 284 132
22	−4.383 389 048	1.424 513 214	−3.361 443 569	5.792 753 946
23	−4.336 970 494	1.416 691 312	−3.224 987 032	5.658 579 334
24	−4.305 279 471	1.411 481 234	−3.101 773 019	5.559 966 820
25	−4.251 393 955	1.402 529 166	−2.928 596 939	5.399 327 527
26	−4.185 092 547	1.391 743 755	−2.668 915 949	5.190 114 130
27	−4.134 393 805	1.383 454 870	−2.491 134 144	5.033 823 177
28	−4.068 857 947	1.372 925 337	−2.218 436 807	4.821 717 645
20	−3.002 625 739	1.19	0.840 158 3251	1.820 134 994
21	−2.989 943 090	1.19	1.064 189 417	1.712 490 790
22	−2.977 800 616	1.19	1.311 181 915	1.603 789 591
23	−2.967 160 395	1.19	1.519 273 404	1.508 779 897
24	−2.956 610 992	1.19	1.755 659 212	1.409 638 571

Table D4. (continued)

n	a_1	$2\nu_1$	a_2	a_3
25	−2.947 756 459	1.19	1.945 718 751	1.326 801 891
26	−2.939 000 159	1.19	2.160 325 380	1.240 761 320
27	−2.931 582 457	1.19	2.333 557 705	1.168 364 089
28	−2.924 319 651	1.19	2.527 044 334	1.093 985 623
20	−3.591 404 322	1.29	−0.951 470 6910	3.514 121 096
21	−3.584 155 248	1.29	−0.827 888 0799	3.453 222 689
22	−3.577 164 741	1.29	−0.681 293 6357	3.390 026 328
23	−3.571 423 036	1.29	−0.573 562 3368	3.339 377 936
24	−3.565 542 637	1.29	−0.437 506 3145	3.283 538 195
25	−3.561 147 627	1.29	−0.347 736 9847	3.243 010 963
26	−3.556 660 462	1.29	−0.233 409 4556	3.198 363 502
27	−3.553 336 603	1.29	−0.160 435 2409	3.166 495 500
28	−3.550 005 621	1.29	−0.067 171 5826	3.131 828 410

Table D5. The coefficients of three fits to the larger eigenvalue, $\lambda_3(n) = \lambda_2(n)$, of the moment of inertia for the (P-P-P) model. The top fit allows the value of ν to be free while the bottom two fits fix this exponent. These fits use $\frac{1}{n}$ corrections: see equation (3.31).

n	a_1	$2\nu_3$	a_2	a_3
20	−2.474 887 010	1.330 133 182	1.169 158 567	1.380 214 814
21	−2.451 727 355	1.324 819 993	0.984 580 2007	2.056 262 136
22	−2.424 625 717	1.318 682 413	0.758 206 4092	3.216 116 413
23	−2.402 331 687	1.313 703 614	0.563 333 8950	4.044 177 082
24	−2.384 502 562	1.309 756 026	0.402 046 4689	4.986 481 513
25	−2.363 446 512	1.305 145 685	0.204 718 825	5.916 901 080
26	−2.345 549 804	1.301 270 237	0.029 444 054	7.025 885 609
27	−2.327 992 403	1.297 496 245	−0.146 489 591	7.927 417 445
28	−2.310 098 163	1.293 691 011	−0.333 726 665	9.196 060 404
20	−1.859 794 757	1.19	−3.860 040 364	23.847 891 60
21	−1.852 652 904	1.19	−4.124 366 246	26.166 264 50
22	−1.846 211 559	1.19	−4.376 201 889	28.737 842 89
23	−1.840 251 622	1.19	−4.620 417 516	31.114 375 93
24	−1.834 780 204	1.19	−4.856 318 771	33.767 638 79
25	−1.829 762 026	1.19	−5.081 959 793	36.180 851 37
26	−1.825 086 009	1.19	−5.302 251 764	38.886 174 00
27	−1.820 788 301	1.19	−5.512 698 552	41.340 742 72
28	−1.816 777 611	1.19	−5.717 671 690	44.070 614 71
20	−2.298 728 754	1.29	−0.271 171 3545	7.814 819 509
21	−2.297 004 286	1.29	−0.334 907 2110	8.283 144 238
22	−2.295 701 309	1.29	−0.386 214 2636	8.904 699 700
23	−2.294 628 149	1.29	−0.429 952 6474	9.231 222 466
24	−2.293 815 488	1.29	−0.465 418 7863	9.734 461 374
25	−2.293 248 258	1.29	−0.490 667 8487	9.897 709 787
26	−2.292 833 438	1.29	−0.510 593 0268	10.252 983 09
27	−2.292 622 533	1.29	−0.520 702 6654	10.257 501 86
28	−2.292 537 860	1.29	−0.525 371 9254	10.437 423 75

(table D5) is clearly unstable with $2\nu_3$ decreasing and the coefficient a_2 changing rapidly. Furthermore, by fixing the value of $2\nu_3$ to 1.29, which is the same as the free estimate of around 1.29, a big change is produced in the coefficient a_2. Better behaved are some of the fits

Table D6. The coefficients of three fits to the largest eigenvalue, $\lambda_3(n) = \lambda_2(n)$, of the moment of inertia for the (P-P-P) model. The top fit allows the value of ν to be free while the bottom two fits fix this exponent. These fits use $\frac{1}{\sqrt{n}}$ corrections: see equation (3.32).

n	a_1	$2\nu_3$	a_2	a_3
20	−2.289 709 609	1.300 873 021	2.156 581 910	−0.641 494 007
21	−2.203 913 210	1.286 015 179	2.372 074 485	−0.875 640 625
22	−2.074 442 935	1.264 311 462	2.811 630 202	−1.260 842 112
23	−2.002 427 148	1.252 107 081	3.013 642 266	−1.465 889 862
24	−1.934 589 619	1.240 977 908	3.276 552 782	−1.677 637 868
25	−1.874 144 773	1.230 877 504	3.457 941 812	−1.854 517 812
26	−1.810 893 738	1.220 664 223	3.722 052 864	−2.058 290 520
27	−1.770 887 298	1.214 043 641	3.844 019 958	−2.177 090 231
28	−1.711 412 712	1.204 558 139	4.107 592 804	−2.373 584 861
20	−1.636 913 110	1.19	4.143 013 210	−2.519 666 678
21	−1.633 379 274	1.19	4.188 757 262	−2.547 008 047
22	−1.629 046 469	1.19	4.292 272 220	−2.588 222 694
23	−1.627 137 319	1.19	4.313 440 217	−2.602 820 328
24	−1.624 169 435	1.19	4.394 573 742	−2.632 908 767
25	−1.623 405 873	1.19	4.395 447 180	−2.637 815 348
26	−1.621 492 277	1.19	4.456 090 152	−2.658 581 094
27	−1.621 394 660	1.19	4.443 674 362	−2.657 516 847
28	−1.620 325 282	1.19	4.485 241 679	−2.670 248 710
20	−2.225 691 696	1.29	2.351 384 151	−0.825 680 5566
21	−2.227 591 431	1.29	2.296 679 775	−0.806 276 1517
22	−2.228 410 599	1.29	2.299 796 592	−0.801 985 9233
23	−2.231 399 964	1.29	2.220 604 371	−0.772 222 2431
24	−2.233 101 073	1.29	2.201 408 356	−0.759 009 2032
25	−2.236 797 036	1.29	2.101 991 533	−0.721 606 3134
26	−2.239 152 583	1.29	2.062 355 258	−0.700 978 8882
27	−2.243 148 807	1.29	1.949 681 393	−0.659 385 4256
28	−2.246 011 252	1.29	1.891 025 753	−0.632 405 9189

in table D6, with the fit using $2\nu_3$ free and that fixing it at 1.19 giving similar results, although not as good as in the $\lambda_1(n)$ analysis. So we can tentatively conclude that, *opposed* to the differential approximant analysis for $\lambda_3(n)$, an estimate of $2\nu_3$ around the SAW value of 1.19, with strong $\frac{1}{\sqrt{n}}$ corrections, is best supported by the data fits. While somewhat debatable, it is certainly *consistent* with the data fits.

References

[1] Madras N and Slade G 1993 *The Self-Avoiding Walk* (Boston: Birkhauser)
[2] Redner S and Majid I 1983 *J. Phys. A: Math. Gen.* **16** L307
[3] Privman V and Švrakić N M 1989 *Directed Models of Polymers, Interfaces, and Clusters: Scaling and Finite-Size Properties (Lecture Notes in Physics vol 338)* (Berlin: Springer)
[4] Grassberger P 1982 *Z. Phys.* B **48** 255
[5] Guttmann A J and Wormald N 1984 *J. Phys. A: Math. Gen.* **17** L271
[6] Joyce G S 1984 *J. Phys. A: Math. Gen.* **17** L463
[7] Whittington S G 1984 *J. Phys. A: Math. Gen.* **17** L117
[8] Blöte H W J and Hilhorst H J 1984 *J. Phys. A: Math. Gen.* **17** L111
[9] Manna S S 1984 *J. Phys. A: Math. Gen.* **17** L899
[10] Whittington S G 1985 *J. Phys. A: Math. Gen.* **18** L67
[11] Guttmann A J and Wallace K J 1986 *J. Phys. A: Math. Gen.* **19** 1645

[12] Guttmann A J, Prellberg T and Owczarek A L 1993 *J. Phys. A: Math. Gen.* **26** 6615
[13] Brak R, Owczarek A L and Soteros C 1998 *J. Phys. A: Math. Gen.* **31** 4851
[14] Guttmann A J and Wallace K J 1985 *J. Phys. A: Math. Gen.* **18** L1049
[15] Enting I G and Guttmann A J 1989 *J. Phys. A: Math. Gen.* **22** 1371
[16] Guttmann A J 1989 *J. Phys. A: Math. Gen.* **22** 2807
[17] Guttmann A J and Wang J 1991 *J. Phys. A: Math. Gen.* **24** 3107
[18] Joyce G S and Brak R 1985 *J. Phys. A: Math. Gen.* **18** L293
[19] Liu K C and Lin K Y 1985 *J. Phys. A: Math. Gen.* **18** L647
[20] Szekeres G and Guttmann A J 1987 *J. Phys. A: Math. Gen.* **20** 481
[21] Nienhuis B 1982 *Phys. Rev. Lett.* **49** 1062
[22] Fisher M E and Sykes M F 1959 *Phys. Rev.* **114** 45
[23] Li B, Madras N and Sokal A D 1995 *J. Stat. Phys.* **80** 661
[24] Caracciolo S, Causo M S and Pelissetto A 1998 *Phys. Rev.* E **57** R1215
[25] Guttmann A J 1989 *Phase Transitions and Critical Phenomena* vol 13, ed C Domb and J L Lebowitz (New York: Academic)
[26] Batchelor M T, Bennett-Wood D and Owczarek A L 1998 *Eur. Phys. J.* B **5** 139
[27] Andrews G E 1976 The theory of partitions *Encyclopedia of Mathematics and its Applications* vol 2, ed G-C Rata (Reading, MA: Addison-Wesley)
[28] Bhatia D P, Prasad M A and Arora D 1997 *J. Phys. A: Math. Gen.* **30** 2281
[29] Conway A and Guttmann A J 1996 *Phys. Rev. Lett.* **77** 5284
[30] Anonymous referee 2000 private communication
[31] Owczarek A L, Rechnitzer A and Wong L H 2000 The anti-spiral self-avoiding walk, in preparation
[32] Rechnitzer A 2000 *PhD Thesis* University of Melbourne, in preparation
[33] MacMahon P A 1960 *Combinatory Analysis* vol 2 (New York: Chelsea) section 8